AD-A113 527 CIVIL ENGINEERING LAB (NAVY) PORT HUENEME CA F/G 8/7
PERMEABILITY AND STRENGTH CHARACTERISTICS OF GRADED CRUSHED STO--ETC(U)
SEP 80 G Y WU NIPR-5-80-12

UNCLASSIFIED ESL-TR-80-54 NL

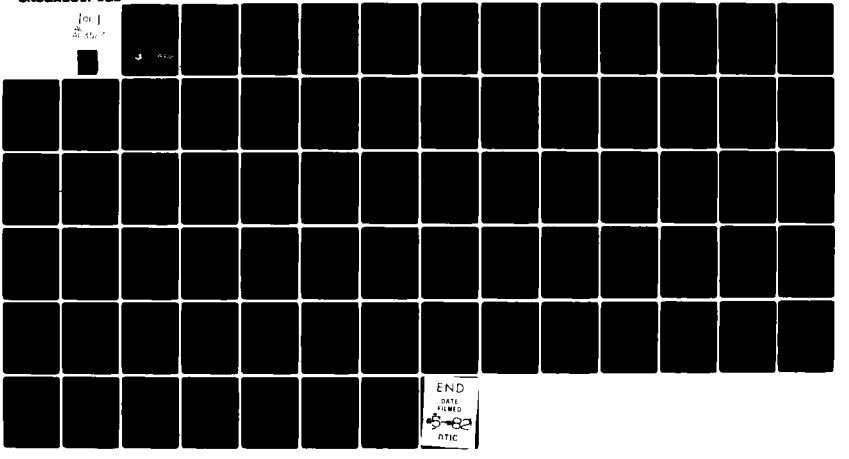

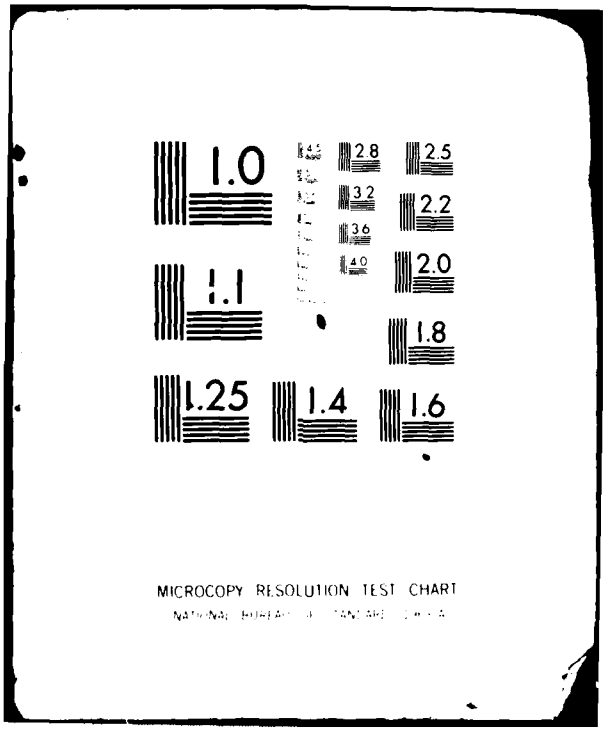
1.0
1.1
1.25
1.4
1.6
1.8
2.0
2.2
2.5
2.8
3.2
3.6
4.0
MICROCOPY RESOLUTION TEST CHART

ESL-TR-80-54

(12)

PERMEABILITY AND STRENGTH CHARACTERISTICS OF GRADED CRUSHED STONE FOR USE IN RAPID RUNWAY REPAIR

G. Y. WU

CIVIL ENGINEERING LABORATORY
NAVAL CONSTRUCTION BATTALION CENTER
PORT HUENEME, CA 93043

SEPTEMBER 1980

FINAL REPORT
JANUARY 1980 TO SEPTEMBER 1980

APPROVED FOR PUBLIC RELEASE: DISTRIBUTION UNLIMITED

AFESC

ENGINEERING & SERVICES LABORATORY
AIR FORCE ENGINEERING & SERVICES CENTER
TYNDALL AIR FORCE BASE, FLORIDA 32403

NOTICE

Please do not request copies of this report from HQ AFESC/RD (Engineering and Services Laboratory). Additional copies may be purchased from:

National Technical Information Service
5285 Port Royal Road
Springfield, Virginia 22161

Federal Government agencies and their contractors registered with Defense Technical Information Center should direct requests for copies of this report to:

Defense Technical Information Center
Cameron Station
Alexandria, Virginia 22314

UNCLASSIFIED

SECURITY CLASSIFICATION OF THIS PAGE *(When Data Entered)*

REPORT DOCUMENTATION PAGE	READ INSTRUCTIONS BEFORE COMPLETING FORM
1. REPORT NUMBER: ESL-TR-80-54	2. GOVT ACCESSION NO.: AD-A113527
3. RECIPIENT'S CATALOG NUMBER	
4. TITLE *(and Subtitle)*: Permeability and Strength Characteristics of Graded Crushed Stone For Use In Rapid Runway Repair	5. TYPE OF REPORT & PERIOD COVERED: Final Report January 1980 - September 1980
6. PERFORMING ORG. REPORT NUMBER	
7. AUTHOR(s): G.Y. Wu	8. CONTRACT OR GRANT NUMBER(s): MIPR S-80-12
9. PERFORMING ORGANIZATION NAME AND ADDRESS: Civil Engineering Laboratory, Naval Construction Battalion Center, Port Hueneme, CA 93043	10. PROGRAM ELEMENT, PROJECT, TASK AREA & WORK UNIT NUMBERS: Program Element: 64708 F, JON: 20546B17
11. CONTROLLING OFFICE NAME AND ADDRESS: Air Force Engineering and Services Center/RDCR, Tyndall Air Force Base Florida 32403	12. REPORT DATE: September 1980
	13. NUMBER OF PAGES: 76
14. MONITORING AGENCY NAME & ADDRESS *(if different from Controlling Office)*	15. SECURITY CLASS. *(of this report)*: Unclassified
	15a. DECLASSIFICATION DOWNGRADING SCHEDULE

16. DISTRIBUTION STATEMENT *(of this Report)*

Approved for public release; distribution unlimited.

17. DISTRIBUTION STATEMENT *(of the abstract entered in Block 20, if different from Report)*

18. SUPPLEMENTARY NOTES

Availability of this report is specified on reverse of front cover.

19. KEY WORDS *(Continue on reverse side if necessary and identify by block number)*

Graded crushed limestone, permeability, pore pressure, friction angle, cohesion, rapid runway repair.

20. ABSTRACT *(Continue on reverse side if necessary and identify by block number)*

The permeability and strength characteristics of six gradations of crushed limestone were evaluated in the laboratory to identify a gradation of crushed limestone that is stronger than the Tyndall gradation. Based on limited laboratory tests, pore pressure buildup did not seem to be a significant problem associated with the crushed limestone. The frictional strength criterion is not suitable for this crushed limestone because the friction angles obtained from undrained triaxial tests may not be valid within the applied

(continued)

DD FORM 1 JAN 73 1473 EDITION OF 1 NOV 65 IS OBSOLETE

UNCLASSIFIED

SECURITY CLASSIFICATION OF THIS PAGE *(When Data Entered)*

20. Continued

range of confining pressures. With the assumption that strength at low confining pressure is more important than at high confining pressure, the cohesion criterion was selected for analyzing tests. Field traffic tests are needed to validate the assumption.

PREFACE

This report was prepared by the Naval Civil Engineering Laboratory (NCEL), Port Hueneme, California, under MIPR S-80-12 from the Air Force Engineering and Services Center (AFESC). The work was begun in January 1980 and completed in September 1980. Mr. George Wu was the principal investigator at NCEL and the AFESC project officer was Lt Ken Knox.

This report has been reviewed by the Public Affairs Office (PA) and is releasable to the National Technical Information Service (NTIS). At NTIS it will be available to the general public including foreign nationals.

This technical report has been reviewed and is approved for publication.

GREGORY T. BEYER, Capt, USAF
Project Officer, BDR

JAMES R. VAN ORMAN, GS-14
Chief, Rapid Runway Repair Branch

JOHN E. GOIN, Lt Col, USAF
Chief, Engineering Research Division

FRANCIS B. CROWLEY III, Col, USAF
Dir, Engineering & Services Laboratory

(The reverse of this page is blank)

CONTENTS

LIST OF TABLES

LIST OF FIGURES

ACKNOWLEDGMENT

The author is grateful to colleagues Dr. James B. Forrest, Research Civil Engineer, for his suggestions and comments; and Mr. John E. Crawford, Research Structural Engineer, for his assistance in finite element analysis.

(The reverse of this page is blank)

SECTION I

INTRODUCTION

The research project reported herein was sponsored by the Air Force Engineering and Services Center (AFESC), Tyndall AFB, Florida., under AFESC/ACB MIPR S-80-12 of 12 December 1979. The objective was to determine the permeability and strength characteristics of graded crushed limestone for use in the USAF rapid runway repair program.

1. BACKGROUND

Research on bomb damage repair (BDR) procedures has been conducted since the mid 1960s to provide the technology to rapidly repair all levels of airfield damage. Continuing improvements in methods of expedient bomb damage repair are needed to meet modern weapons threats.

The AFESC has been conducting material studies and field tests on expedient repair of bomb-damaged runways. AFESC demonstrated that a 24-inch layer of crushed limestone, compacted only from the surface by a 10-ton vibratory roller, is capable of carrying F-4 wheel loads (Ref 1). However, it was found that the compacted crushed stone layer is very sensitive to excess moisture. In loadcart field tests, rutting failures occurred whenever the moisture content of the compacted crushed stone layer exceeded 5.4%. AFESC reported that rutting failures seemed to be the result of excess pore pressures which were caused by the very low permeabilities of the compacted base course materials.

In 1967, the Waterways Experiment Station (WES) had examined the drainage characteristics of highly compacted base course materials. WES recommended that a maximum of 5% of fines be specified for base course materials (Ref 2). Earlier in 1962, the National Crushed Stone Association (NCSA) studied the effects of the various characteristics of base course materials on the strength of the materials (Ref 3). NCSA determined that the percent of fines has a significant influence on the strength of the base course material. NCSA further concluded that 5% to 12% fines is required for maximum strength.

Consequently, the Naval Civil Engineering Laboratory (NCEL) was requested to conduct a laboratory investigation to determine the permeability and strength characteristics of graded crushed stone for use in expedient repair of bomb-damaged runways. The objective was to identify a gradation, if any, that would resist pore pressure buildup when the crushed stone is saturated and have the capability of supporting F-4 wheel loads of 27,000 pounds at 265 psi tire pressure. A major benefit of this laboratory study of crushed stone would be the cost saving relative to conducting full-scale field tests. With the assistance of a very limited amount of field test data available, the study was conducted to identify crushed stone gradations which are stronger than that used in the field loadcart tests, and to determine their pore pressure characteristics when loaded.

2. SCOPE OF STUDY

The study was carried out to support an on-going research project on expedient bomb-damaged runway repair by the AFESC. It was mainly intended to identify a gradation of crushed limestone that is stronger than the Tyndall gradation (Gradation No. 1), which had been tested at high moisture contents and failed. A substantial savings in time and money could result by eliminating crushed limestone gradations that are weaker than the Tyndall gradation used for the loadcart field test. Another purpose of this study was to obtain a better understanding of the drainage and strength characteristics of compacted crushed limestone as measured by permeability and triaxial tests in the laboratory.

The following tests were conducted on a total of six gradations of crushed stone in the laboratory to determine the permeability and strength characteristics of compacted crushed limestone:

a. Constant head permeability

b. Undrained triaxial

c. Atterberg limit

d. Soundness

e. Wear

f. Compaction

g. Maximum and minimum densities

SECTION II

LABORATORY TESTING AND DATA REDUCTION

1. GENERAL SOIL DESCRIPTION

The crushed limestone tested was shipped to NCEL from Tyndall AFB FL. The crushed stone was subangular to angular in shape and appeared to have a uniform density. At least 75% of the particles retained on a 3/8-inch sieve had two or more fracture faces. The crushed stone, coated with fine silty particles, had the appearance of sound and durable particles. It was light gray in color and blended with a small amount of sea shell fragments.

2. GRAIN SIZE ANALYSES

Grain size analyses were performed in accordance with American Society for Testing Materials (ASTM) Standard C136 for dry sieving. All the plus 1-1/2-inch sieve materials were removed before sieve analysis and laboratory tests. The grain size distribution curves for all gradations tested are presented from Figures 12 to 17. Grain size distribution of the crushed stone also was determined after triaxial shear tests, and after Modified Proctor compaction tests in the laboratory.

A typical grain size distribution curve for a sample after one CE-55 compaction test is illustrated in Figure 1. It seems that particle degradation caused by impact compaction was more pronounced on particles greater than the no. 10 sieve (2.0 mm). There was no noticeable increase in the amount of fines after the compaction test. The grain size distribution for the same gradation after static compaction and triaxial undrained tests is shown in Figure 2. There was only a slight difference between the curves obtained before and after triaxial tests. This supported the assumption that static compaction plus vibration would not cause substantial particle degradation.

3. ATTERBERG LIMITS

In accordance with ASTM procedures, plastic limit tests were attempted on the portion of crushed stone passing through the no. 40 sieve. The crushed limestone was classified as nonplastic when a 1/8-inch-diam soil thread could not be developed.

To further investigate the properties of the crushed limestone, a liquid limit test was performed on the portion of crushed stone passing through the No. 200 sieve. The liquid limit of the particles passing through the No. 200 sieve was about 20.5% water content, as indicated in Figure 3. The corresponding plastic limit of the fines was about 15% water content.

It was concluded that the crushed limestone was basically classified as nonplastic, but it contained plastic fines.

4. IMPACT COMPACTION TEST

Impact compaction tests, as described in MIL-STD-621A (Ref 4), were performed to determine the moisture-density relationship for each gradation of crushed stone. A brief description of the procedure is listed below:

Volume of Mold	=	0.07 ft^3
Number of Layers	=	5
Weight of Hammer	=	10 pounds
Height of Hammer Drop	=	18 inches
Number of Blows/Layer	=	55
Total Energy	=	55,000 ft-lb/ft^3

Particles greater than 3/4 inch were first removed and replaced with an equal percentage by weight of material passing 3/4 inch and retained on the no. 4 sieve. The percentage of material finer than the no. 4 sieve therefore remained constant.

The moisture-density relationship for gradation Nos. 1 to 6 are presented from Figures 4 to 9, respectively. The moisture-density curves indicate that the dry densities of the materials were rather independent of the moisture content used. This appeared to be valid at least up to the optimum moisture content. A summary of compaction results for all gradations is presented in Table 1.

Table 1. CE-55 Compaction Test Results

Gradation No.	Maximum Density (pcf)	Optimum Moisture Content (%)
1	141.1	5.9
2	143.4	5.1
3	145.3	2.8
4	136.5	1.5
5	128.3	3.1
6	116.9	1.5

The compaction test was stopped whenever a substantial amount of water had drained out of the compaction mold. The draining of water from the compaction mold suggested that the crushed stone could absorb no more water. Any additional amount of water would consequently be drained away. Furthermore, there were questions on whether the impact compaction test is applicable to coarse crushed stone. For gradations with very little or no fines, the coarse aggregates would merely move around and would not get compacted. The addition of more water than the stone could absorb would have no significant effect on the compaction results. In fact, coarse aggregates were found to be rather insensitive to moisture and the resulting compaction curves were essentially flat.

5. MAXIMUM AND MINIMUM DENSITY

In addition to impact compaction tests, maximum and minimum density tests were performed by the following procedures. Approximately 700 grams of soil was put in a 1,000-cc plastic graduated cylinder. The minimum dry density in a dry state was determined by slowly rotating and turning the graduated cylinder from end to end to put the soil into the loosest state. The maximum dry density in a dry state was obtained by vigorously vibrating the outside of the plastic graduated cylinder with a pneumatic vibrating hand tool. The maximum and minimum dry densities in a wet state were obtained in the same way, except water was added to the plastic graduated cylinder to the 1,000-cc mark. The results of these maximum and minimum density tests for gradation no. 4 are listed below:

Minimum Dry Density in a Dry State = 98.4 pcf
Maximum Dry Density in a Dry State = 109.1 pcf
Minimum Dry Density in a Wet State = 81.0 pcf
Maximum Dry Density in a Wet State = 109.1 pcf

The maximum dry density of 136.5 pcf, as obtained by the CE-55 impact compaction test, was considerably greater than that of 109.1 pcf obtained by vibration. It was noted that impact compaction caused particle breakdown whereas vibration would almost preclude tendency for particle breakdown. The relationship between relative density and dry density for gradation no. 4 is illustrated in Figure 10. The maximum and minimum densities were only used to establish the relative density curve.

6. SOUNDNESS TEST

The purpose of soundness tests was to determine the resistance of crushed limestone to disintegration by saturated solutions of sodium sulfate. The test results provide helpful information in judging the soundness of aggregates subject to weathering action. The soundness tests were performed in accordance with ASTM Standard C88 (Ref 5). The test results are listed below.

Soundness Test by Use of Sodium Sulfate

Particle Size	Percentage Loss of Size	Percentage Size in Sample	Weighted Average (%)
3/8 inch to no. 4	0.5	76	0.38
no. 4 to no. 8	0.5	24	0.12
Total Loss			0.50

7. ABRASION TEST

The abrasion test is a procedure for testing the resistance of coarse aggregate to abrasion, using the Los Angeles testing machine. The test was conducted in accordance with ASTM procedure C131 (Ref 5). The abrasion test results are:

Loss at 100 Revs = 5.2%
Loss at 500 Revs = 23.5%

8. STONE SAMPLING

A total of approximately 4,000 pounds of crushed limestone was received from AFESC, Tyndall AFB, Fla. The soil particles were first dried in a rotary kiln and then sieved into different grain sizes. This was bound to be the most accurate and precise way fulfilling the gradation requirement. The sieved soil particles were stored in cans.

SECTION III

PERMEABILITY AND UNDRAINED TRIAXIAL TESTS

It has been suggested that the strength of soil specimens might be affected by parameters such as the particle size, the amount of fines, the permeability of the material, the size of specimens, and the method of sample preparation. For the latter factor, the difference in strength could sometimes be more than 100% (Ref 6).

The present study was carried out to determine the drainage and strength characteristics of graded crushed limestone for use in the Rapid Runway Repair Program. The laboratory test program consisted of constant head permeability and undrained triaxial tests on each crushed stone specimen. The equipment setup is illustrated in Figure 11. A Tinus-Olsen loading frame with an automatic cyclic loading capability was used. The triaxial chamber was positioned inside the loading frame. Axial load was measured by a load cell and axial strain was measured by an Linear Voltage Displacement Transducer (LVDT). The test data were recorded by a multichannel Honeywell Viscorder model no. 1858. In the foreground of Figure 11 from left to right are pneumatic vibrator, electric concrete vibrator, compaction pedestal, compaction mold, and membrane stretcher.

The confining pressure used in all triaxial tests ranged from 10 psi to 120 psi. Confining pressure greater than 120 psi was not used because the most critical zones were the soil near the edges of the wheel, not directly beneath it. The maximum stress near the edge of the wheel was reduced to some fraction of the total wheel stress, depending on distance from the edge.

1. TRIAXIAL SAMPLE PREPARATION METHOD

A number of techniques have been commonly used to prepare specimens for triaxial testing. Static compaction plus vibration was chosen for the present crushed limestone test program. The selection was based on the finding that static compaction plus vibration caused the least amount of particle degradation, when compared to impact compaction techniques. In addition, static compaction plus vibration simulated closely the vibratory roller compaction applied in the field.

Static compaction plus vibration involved the use of a pneumatic tool and static load. Before each layer of crushed stone was compacted, an electric concrete vibrator was utilized to "rod" the stone. The stone surface was leveled and a static load was applied. A pneumatic vibrating hand tool was also used to vibrate the outside of the mold while the static load was increasing. In order to minimize the crushing of stone particles, the following procedure was used. When the static load applied on the specimen reached a predetermined value, the static load was released to almost zero. The sample was then reloaded and unloaded. The same process was repeated until the targeted height of 12 inches was obtained. During this compaction process, the height of the sample was carefully monitored to avoid overcompaction.

The specimens were prepared in a split mold attached to the bottom pedestal of the triaxial cell and were compacted to the desired dry density at slightly above optimum moisture content. The triaxial specimens were 6 inches in diameter and 12 inches tall. Detailed triaxial test prodedures have been described in an earlier report (Ref 7). The test procedures used in the present study closely followed the standard procedures (Ref 7) but with modified steps to treat crushed limestone. A brief procedure description is presented below.

The graded material was first recombined to conform to the gradation requirement. The maximum particle size used was 1-1/2 inches. De-aired water was then added to the material to about 1% above the optimum water content and the material was allowed to cure overnight. Normally, the maximum recommended thickness for each soil layer should not exceed 1 inch. Due to the size of the particles involved, the specimens were compacted in four equal layers of about 3 inches each. A 0.025-inch-thick latex membrane was placed on the inside wall of the compaction mold to prevent specimens from crumbling when the mold was removed. An additional 0.025-inch-thick layer of latex membrane and a final 0.06-inch-thick layer of butyl membrane were applied to surround the sample after the specimen was compacted and the mold was removed.

Rubber O-rings were utilized to seal the membrane around the cap and base. Porous stone plates and filter paper discs were used between the specimen and its cap and base.

As soon as the sample was placed in the triaxial cell and surrounded by membranes, a vacuum of about 0.8 atmosphere was immediately applied to the sample while the cell chamber was being assembled and filled with de-aired water. The following method was employed to saturate specimens. Under a confining pressure of about 2 psi, de-aired water was fed in from the bottom drainage line through the sample and pulled out from the top drainage line under vacuum. This de-aired water flushing process continued until no visible air bubbles were present in the pore line.

2. PERMEABILITY TEST

After saturation, the specimen was subjected to a constant head permeability test. Water was fed in from the top drainage line, 1/4-inch in diameter, and came out from the bottom drainage line, 1/4-inch in diameter. After a sufficient amount of water was collected in the graduated cylinder for a satisfactory measure of its volume, the bottom drainage line was connected to a differential pore pressure transducer for the loading test. During the permeability tests, the head loss caused by tube friction was not considered to have any significant effect upon the test results. This was because the same system without soil specimen inside was many times more permeable than the system with the most permeable specimen. Furthermore, the main objective of these permeability tests was to compare the permeability of the different gradation samples. As long as the procedure used in each test was the same, a relative indication of soil permeability and a valid comparison could be made.

The next step was to increase the cell pressure to the desired confining pressure with the pore lines open. Just before the axial load was applied, the pore lines were shut off to check for leakage in the system. The sample was then loaded at a constant rate of 0.02 in./min in an undrained condition. Axial stress, axial strain, and pore water pressure were recorded during loading.

3. FAILURE CRITERIA FOR TRIAXIAL TESTS

When a soil specimen is subjected to compressive loading, it initially tends to decrease in volume. In an undrained triaxial test on a saturated soil for which volume change cannot occur, this tendency for volume decrease results in an increase in the pore water pressure. Liquefaction occurs if the pore water pressure reaches the confining pressure. There are many factors, including the degree of saturation and membrane penetration effect in laboratory tests, which may influence the buildup of pore water pressure. Nevertheless, it was believed that when all specimens were tested with the identical procedure, these secondary factors would have relatively similar effect on all specimens.

The stone samples tested were of dense materials (at least 97% CE-55 maximum density). A false peak stress was very unlikely. For analytical purposes, the strength of the crushed stone was defined as the axial stress causing 2% axial strain or the peak stress if the corresponding axial strain was less than 2%. In all cases, 2% axial strain was sufficient for the stress-strain curves to flatten out.

4. "CYCLIC" TRIAXIAL TESTS

In one series of triaxial tests, the specimens were cyclically loaded to determine the accumulative deformation of the sample. The series consisted of samples from gradations 2 and 4. The specimen was first axially loaded to a predetermined stress level and then unloaded to zero. The specimen was cycled in this manner until the measured plastic deformation became negligible. Earlier triaxial compression test data indicated that the gradation no. 4 samples were substantially stronger than the gradation no. 2 samples at low confining pressures (see section on INTERPRETATION OF TRIAXIAL TEST DATA). The cyclic load selected was 90% of the minimum compressive strength measured on gradation No. 2, the weaker of the two gradation samples. The cumulative strain measurement might be helpful in analyzing the crushed stones.

SECTION IV

INTERPRETATION OF TRIAXIAL AND PERMEABILITY TEST DATA

Triaxial test specimens were prepared in a forming mold by static loading plus vibration. The samples were 6 inches in diameter and 12 inches tall. Altogether, seven series of cyclic triaxial tests numbered A to G were performed to obtain the strength properties of the soil. The grain size distribution curves for Series A to F are presented in Figures 12 to 17, respectively. The grain size in Series G was the same as in Series B and D. Triaxial test data are presented in the appendix. The triaxial test results are summarized in Table 2.

Table 2. Summary Table of Triaxial and Permeability Tests

Series	Grad. No.	Percentage of Maximum Density	Percentage Passing No. 200 Sieve	Average Permeability (cm/sec)	Friction Angle (deg)	Apparent Cohesion[a] (psi)
A	1	97	7	9.0×10^{-4}	31	0
		100	7	1.2×10^{-4}	31	27
		103	7	1.2×10^{-4}	31	58
B	2	100	10	5.3×10^{-5}	37	11
C	3	100	5	2.8×10^{-3}	36.5 to 39	30
D	4	97	0	1.5×10^{-2}	29	45
		100	0	6.8×10^{-2}	26.5	52
		103	0	1.7×10^{-2}	25.5	80
E	5	100	0	1.5×10^{-2}	23.5	22
F	6	103	0	2.0×10^{-2}	15	65
G[b]	2,4	100	10	1.3×10^{-5}	38.6	11
		100	0	2.0×10^{-2}	29.8	52

[a]The cohesion obtained by assuming straight line Mohr failure envelope.

[b]Cyclic triaxial tests.

1. FRICTION ANGLE CRITERIA

Other than normal data scattering, Figure 18(a) illustrates the effect of fines on the soil internal friction angle for all gradations. There seems to be a trend that the internal friction angle increases with increasing amount of fine content, regardless of density. Figure 18(b) shows the trend that the apparent cohesion of the crushed stone, as obtained by treating the Mohr failure envelope as a straight line through the intercept, decreases with increasing amount of fines. It was noted that the straight line Mohr envelope method was utilized only for comparing the apparent cohesion of the various gradation samples. It did not necessarily indicate the true internal friction angle of the soil.

The crushed stone in Series A was gap graded. In general, well-graded material is more desirable than gap-graded material for compacted fill. The internal friction angles for Series A were the same from 97% to 103% maximum density. The internal friction angles for Series B, C, and E at 100% maximum density were 37 degrees, 36.5 degrees, and 23.5 degrees, respectively. In Series D, however, the internal friction angle of the material decreased with increasing density. This was in contradiction with the expected finding that dense material is stronger and has larger internal friction angles than that of loose material. In fact, the shear strength of the material, as expressed by the Mohr-Coulomb law, is proportional to the tangent of the internal friction angle:

$$\tau_{ff} = c + \sigma_{ff} \tan \phi$$

where τ_{ff} = shear stress on the failure plane at failure

c = cohesion

σ_{ff} = normal stress on the failure plane at failure

Based on the frictional strength criterion only, the results in Series D suggest that the material compacted to 97% maximum density is stronger than that compacted to 103% maximum density. The internal friction angles at 97% and 103% maximum density were 29 degrees and 25.5 degrees, respectively. However, this is misleading. The above phenomenon was probably due to the fact that the maximum shear strength of the dense crushed stone sample tested at low confining pressure was substantially greater than that of the less dense sample. At high confining pressures, the difference in shear strength between the dense and the loose samples was comparatively smaller than that obtained at low confining pressures. Thus, the straight line Mohr-Coulomb fitting procedure indicated lower friction angles for the stronger material. Another possible explanation is that at low confining pressures, the edges and the corners of the particles create interlocking frictional resistance which is strongly influenced by density. At high confining pressures, interlocking action is more a function of confining stress than density per se. That is also why the shear strength of the material at high confining pressures was not proportionally stronger than that obtained at low confining pressures.

It has been suggested that preloading, friction, and dilation could affect the strength of soil and cannot be analyzed separately (Ref 8). Within the range of the confining pressures used, it appears that the resulting soil internal friction angle may not be valid. Confining pressures higher than those used in this study must be employed in order to avoid the influence of apparent cohesion on the soil friction angle, as illustrated in Figure 19. Since the frictional angle strength criteria cannot be used in this analysis, a different analytical approach is needed. Therefore attention was directed to the apparent cohesion and accumulative strain criteria.

2. COHESION CRITERIA

When a compacted layer of crushed stone is under an F-4 wheel load, the most critical location is the area around the wheel, not underneath it. This is because the area underneath the wheel has high confining stress and the area around the wheel has little or no confining pressure.

By examining the Mohr-Coulomb equation, $\tau_{ff} = c + \sigma_{ff} \tan \phi$, it can be seen that when the confining pressure is small, the shear strength of the sample is approximately equal to the cohesion of the soil. Based on the assumption that the strength of material at low confining pressure is more important, cyclic triaxial test Series G was performed. As indicated in Figure 20, the resistance to deformation of the coarse sample (gradation no. 4), as measured by the cumulative axial deformation caused by a constant cyclic load, was substantially greater than that of the fine sample (gradation no. 2). Based on limited cyclic triaxial test data from Series G, the coarse gradation no. 4 seems to have greater capacity to resist deformation than the fine gradation no. 2.

3. PERMEABILITY EFFECTS

The permeability of the crushed stone is strongly influenced by the amount of fine content, as indicated in Table 2. The difference in permeability between samples with 0% and 10% fines could be as high as three orders of magnitude. It appears that the apparent friction angle of the crushed stone increases with increasing amount of fine content, but decreases with increasing permeability.

The engineers at AFESC reported that a quivering surface was observed when the compacted crushed stone layer was subjected to traffic tests (Ref 1). The quivering surface was thought to be caused by excessive pore pressure buildup. However, based on limited laboratory triaxial tests, no significant increase in pore pressure was measured. In fact, in all series of triaxial tests, pore pressure buildup did not seem to be a major problem. The maximum increase in pore pressure was less than 15% of the confining pressure. The following are possible explanations for the quivering surface phenomenon:

a. Dense samples tend to dilate when sheared, which in turn, allows water to move in and form a quivering surface.

b. After compaction, the fines in the material have negative pore pressures which would allow water to soak in.

c. Wetting effect, i.e., lubrication of sliding surfaces

d. Pumping action occurs anywhere there are fines and water.

By employing the apparent cohesion and accumulative deformation criteria, gradation no. 4 of Series D was found to be the most favorable gradation in terms of cohesion, accumulative strain, and permeability. Based on limited laboratory triaxial tests, the permeability of the crushed stone did not seem to be a major problem since no pore pressure buildup was apparent. The disagreements between laboratory and field observations may indicate inadequate modeling. An essentially static triaxial test in the laboratory may not be appropriate to simulate the loading phenomenon generated by high pressure aircraft tires in the field.

Based on the assumption that strength at low confining pressure is more important, gradation no. 4 seems to be the best material for crushed stone runway repair as explained in the COHESION CRITERIA section. However, actual field tests are necessary to validate this conclusion. There is also a possibility that none of the crushed limestone gradations are strong enough to support F-4 wheel loads. If this turns out to be the case, a different kind of material, or the use of stabilizers or surfacings, may be required to provide support. Further investigation is recommended in this area.

During future loadcart traffic tests in the field, it is recommended that a thin layer of colored sand be placed between every 3 to 6 inches of compact crushed limestone so that the yield profile and, therefore, the failure mechanism can be determined by trenching after the test.

SECTION V

COMPUTER FINITE ELEMENT ANALYSIS

1. DISCUSSION OF COMPUTER MODEL

The computer finite element program selected for the present crushed stone study was ADINA. It is a general purpose finite element program for the analysis of two-dimensional and three-dimensional elastic and inelastic structures subject to static and dynamic loads (Ref 9). The purpose of performing computer finite element analysis was to determine the response of the pavement section under 265 psi F-4 wheel load and to conduct a parameter study to illustrate the comparative effect of cohesion, internal soil friction angle, Young's modulus, and Poisson's ratio. It should be noted that this program cannot produce the exact loading condition that exists in the field, but it can provide comparative information on the response of pavement under load. The reliability of the computer solution depends on the accuracy of the input parameters. Accuracy is usually not a main concern in parameter studies. A ±10% accuracy is generally acceptable.

The soil model utilized was the Drucker and Prager model. It is nonlinear and elastoplastic. The finite element mesh used for the pre sent analysis is presented in Figure 21. Axial symmetry allows the analysis of a radial slice of the pavement section. There were two types of materials employed in the model: a 24-inch layer of compacted crushed stone (material no. 1) and an 8-foot layer of clay (material no. 2), as indicated in Figure 22. The midside node display and the node point numbers are presented in Figures 23 and 24, respectively.

2. RESULTS OF COMPUTER ANALYSIS

The computer results from the computer case study are presented in Table 3.

Table 3. Computer Finite Element Results

Model No.	E (psi)	$\nu = \varepsilon_h/\varepsilon_v$	c (psi)	ϕ (deg)	δ_{max} (in.)	C/L $\sigma_{y\ max}$ (psi)	$\sigma_{xy\ max}$
1	30,000	0.25	11	37	0.18	218	52
2	30,000	0.49	11	37	0.16	273	84
3	30,000	0.25	40	37	0.15	287	75
4	30,000	0.25	11	27	0.21	199	70
5	6,000	0.25	11	37	0.60	204	85

where E = Young's Modulus

ν = Poisson's Ratio

c = cohesion

ϕ = internal friction angle

δ_{max} = maximum deflection

C/L $\sigma_{y\ max}$ = maximum stress along the centerline

$\sigma_{xy\ max}$ = maximum shear stress on the xy plane

In order to determine if the subbase material has any effect on the crushed stone layer during loading, a clay layer beneath the crushed stone layer was employed in the soil models.

The clay layer was assumed to have a Young's modulus of 2,000 psi, a Poisson's ratio of 0.40, a cohesion of 18 psi, and a friction angle of 0 degree (Ref 15).

As shown in Table 3, the material model is most sensitive to the change in Young's modulus. As Young's modulus was decreased from 30,000 psi to 6,000 psi, the corresponding elastic and plastic deformation was increased from 0.18 inch to 0.6 inch. When the cohesion of the material was increased from 11 psi to 40 psi, the corresponding deformation was decreased from 0.18 inch to 0.15 inch. When the friction angle went down from 37 degrees to 27 degrees, the amount of deformation increased from 0.18 inch to 0.21 inch. In addition, the amount of deformation decreased with increasing values of Poisson's ratio.

The computer output also indicates that the clayey subbase material was also affected by the applied wheel load of 27 kips. The relationship of vertical displacement along the centerline of wheel load versus depth and fraction of applied wheel load for soil model no. 5 is shown in Figure 25. Figure 26 illustrates the relationship of vertical displacement on the surface of crushed stone versus distance away from the centerline of loading and fraction of total wheel load for soil model no. 5. Figure 27 shows the relationship of the displacement along the interface of crushed stone and clay layers at a depth of 24 inches versus the distance from the centerline of loading and fraction of total wheel load for soil model no. 5. This indicates why it is important to obtain the exact failure profile in the field to determine if rutting failure was caused by subbase failure.

SECTION VI

CONCLUSIONS AND RECOMMENDATIONS

The objective of this study was to determine the permeability and strength characteristics of graded crushed limestone for use in the USAF rapid runway repair program. The principal conclusions which can be drawn are as follows:

1. Pore water pressure buildup did not seem to be a significant problem associated with the crushed limestone, based on limited laboratory tests. The disagreements between laboratory and field observations may indicate inadequate modeling. An essentially static triaxial test in the laboratory may not be appropriate to simulate the loading phenomenon generated by high pressure aircraft tires in the field.

2. Frictional angle strength criterion is not suitable for the present crushed limestone study. This is because the friction angles obtained by undrained triaxial tests may not be valid within the applied range of confining pressures.

3. With the assumption that strength at low confining pressure is more important than at high confining pressure, the cohesion criterion was selected for the present analysis. Subsequently, gradation D was chosen as the best of the six gradations tested, based on the apparent cohesion and stiffness of the laboratory samples. *Field traffic tests are necessary to validate this assumption.*

Recommendations are as follows:

1. If further testing of crushed limestone is undertaken, it is recommended that a thin layer of colored sand be placed between each layer of compacted crushed limestone so that the rutting failure mechanism (profile) can be determined.

2. Gap-graded material or material having a uniformity coefficient smaller than 4 are not recommended for bomb crater backfill surfacing.

REFERENCES

1. Air Force Engineering and Services Center. MIPR No. S-80-12: Program introduction, BDR crushed stone laboratory study. Dec 1979.

2. Army Engineer Waterways Experiment Station. Technical Report No. 3-786: Drainage characteristics of base course materials laboratory investigation, by E. H. Nettles and C. C. Calhoun. Jul 1967.

3. J. E. Gray. "Characteristics of graded base course aggregates determined by triaxial tests," National Crushed Stone Association, Engineering Bulletin No. 12, Jul 1962.

4. Department of Defense. MIL-STD-621A: Test method for pavement subgrade, subbase, and base-course materials. Dec 1964.

5. American Society for Testing and Materials. 1979 annual book of ASTM standards, part 15. Road, paving, bituminous materials, skid resistance.

6. University of California, College of Engineering. Report No. EERC-75-18: The effect of method of sample preparation on the cyclic stress-strain behavior of sands, by J. P. Mulilis, C. K. Chan, and H. B. Seed. Berkeley, Calif., Jul 1975.

7. Civil Engineering Laboratory. Technical Memorandum M-53-79-11: Cyclic triaxial test procedures for dynamic soil strength evaluation, by G. Y. Wu. Port Hueneme, Calif., Sep 1979.

8. M. J. Hvorslev. "Physical components of the shear strength of saturated clays," ASCE Research Conference on Shear Strength of Cohesive Soils, University of Colorado, Boulder, Colo., Jun 1960.

9. Massachusetts Institute of Technology. Report No. 82448-1: ADINA, a finite element program for automatic dynamic incremental nonlinear analysis, by B. Klaus-Jürgen. Revised Dec 1978.

10. Civil Engineering Laboratory. Technical Note N-1546: Investigation of chemical binders for beach sands, by T. Roe, Jr., S. Tuccillo, and R. Lorenzana. Port Hueneme, Calif., Feb 1979.

11. N. D. Marachi, C. K. Chan, and H. B. Seed. "Evaluation of properties of rockfill materials," *Journal of Soil Mechanics and Foundation Division*, American Society of Civil Engineers, vol 98, no. SM1, Jan 1972, pp 95-114.

12. J. C. Jaeger and G. W. Cook. Fundamentals of rock mechanics. London, England, Methuen and Co., Ltd.

13. H. Cedergren. Drainage of highway and airfield pavements. John Wiley and Sons, Inc., 1974.

14. Civil Engineering Laboratory. Technical Note N-1324: Soil mechanics and the advanced computer codes, by J. B. Forrest. Port Hueneme, Calif., Apr 1974.

15. _____. Technical Note N-1572: Traffic testing of a fiberglass-reinforced polyester resin surfacing for rapid runway repair, by P. S. Springston. Port Hueneme, Calif., Feb 1980.

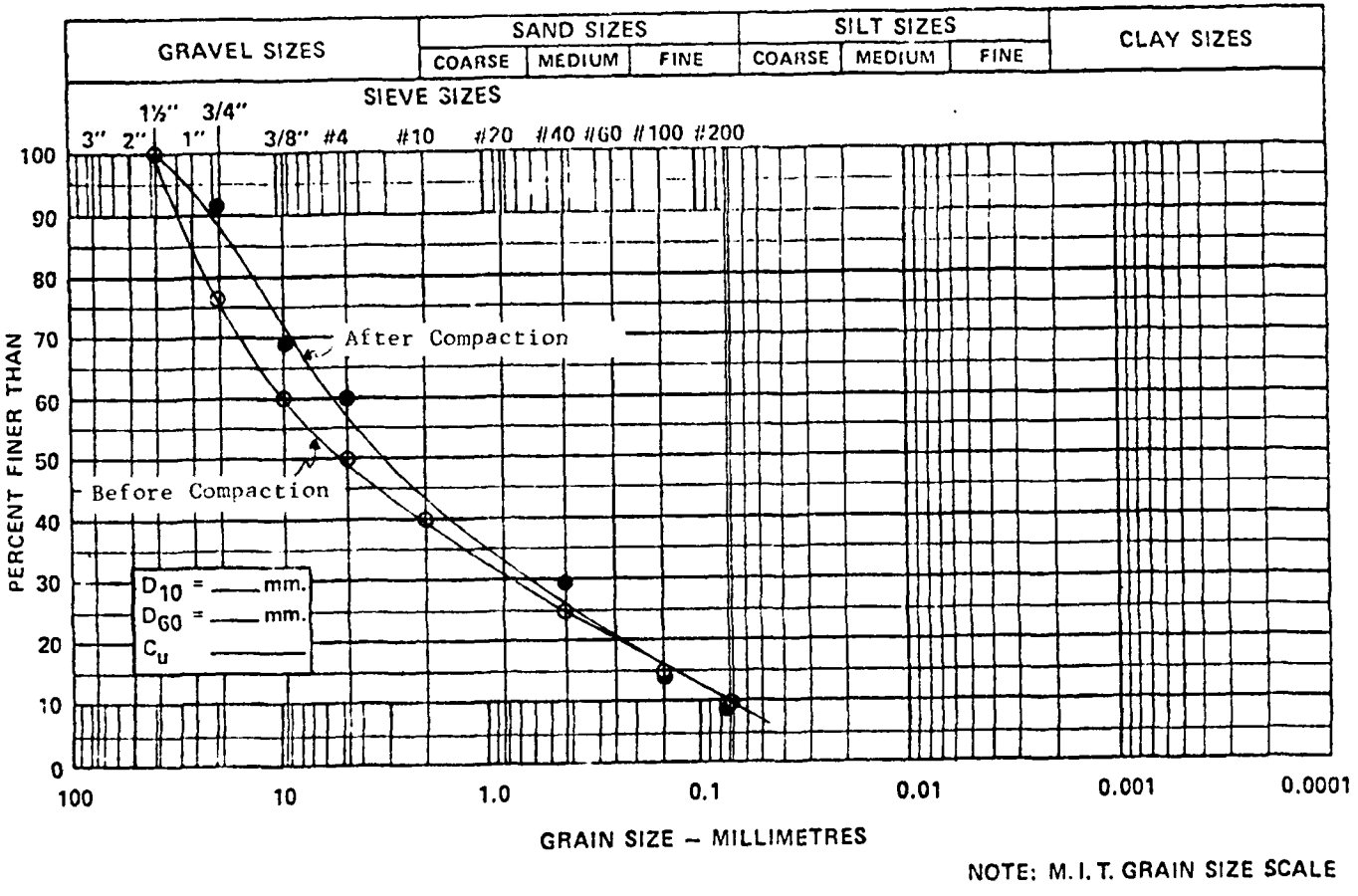

Fig. 1 Typical Grain Size Distribution Curves Showing the Effect of Impact Compaction.

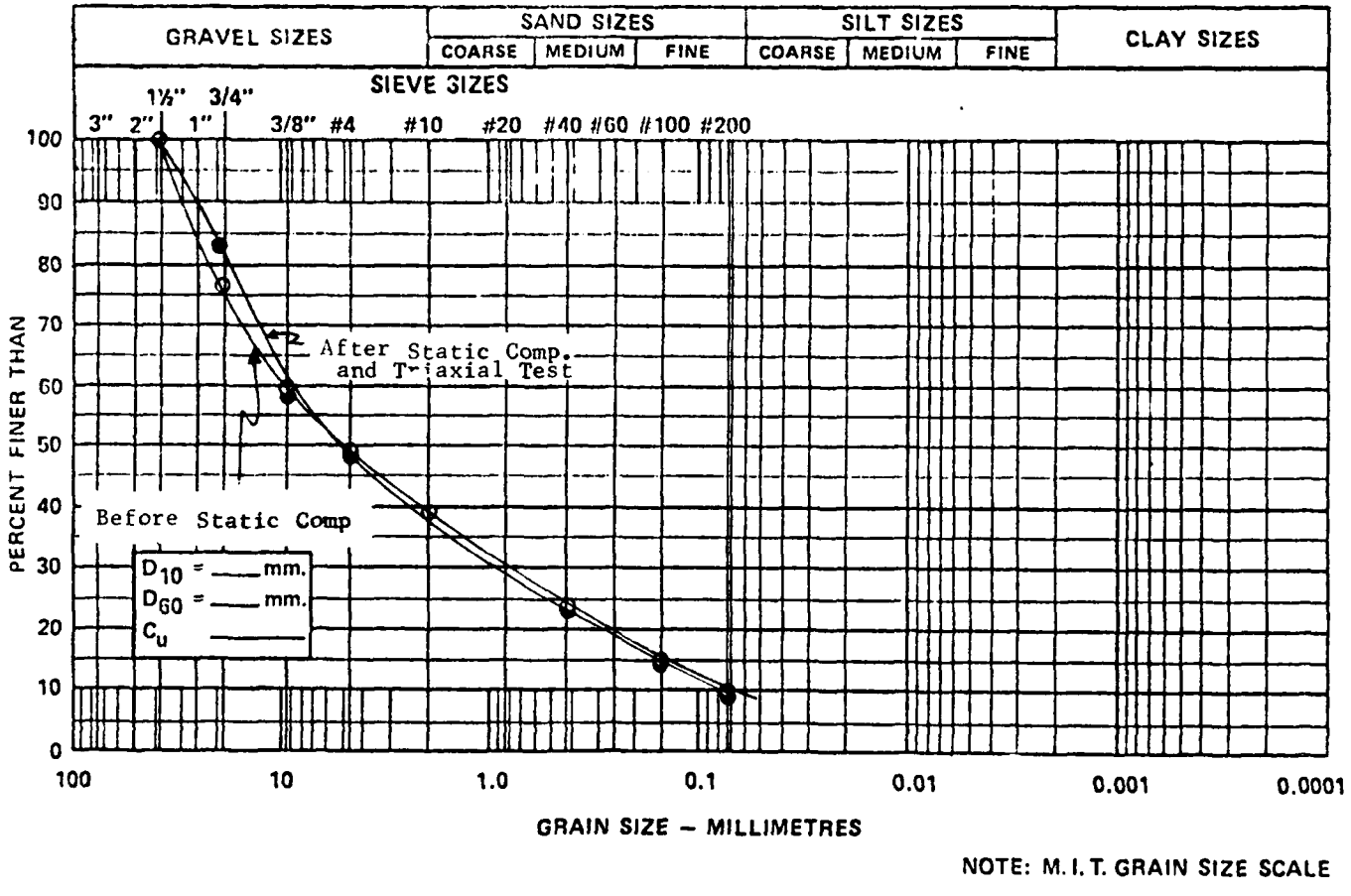

Fig. 2 Typical Grain Size Distribution Curves Before and After Triaxial Test.

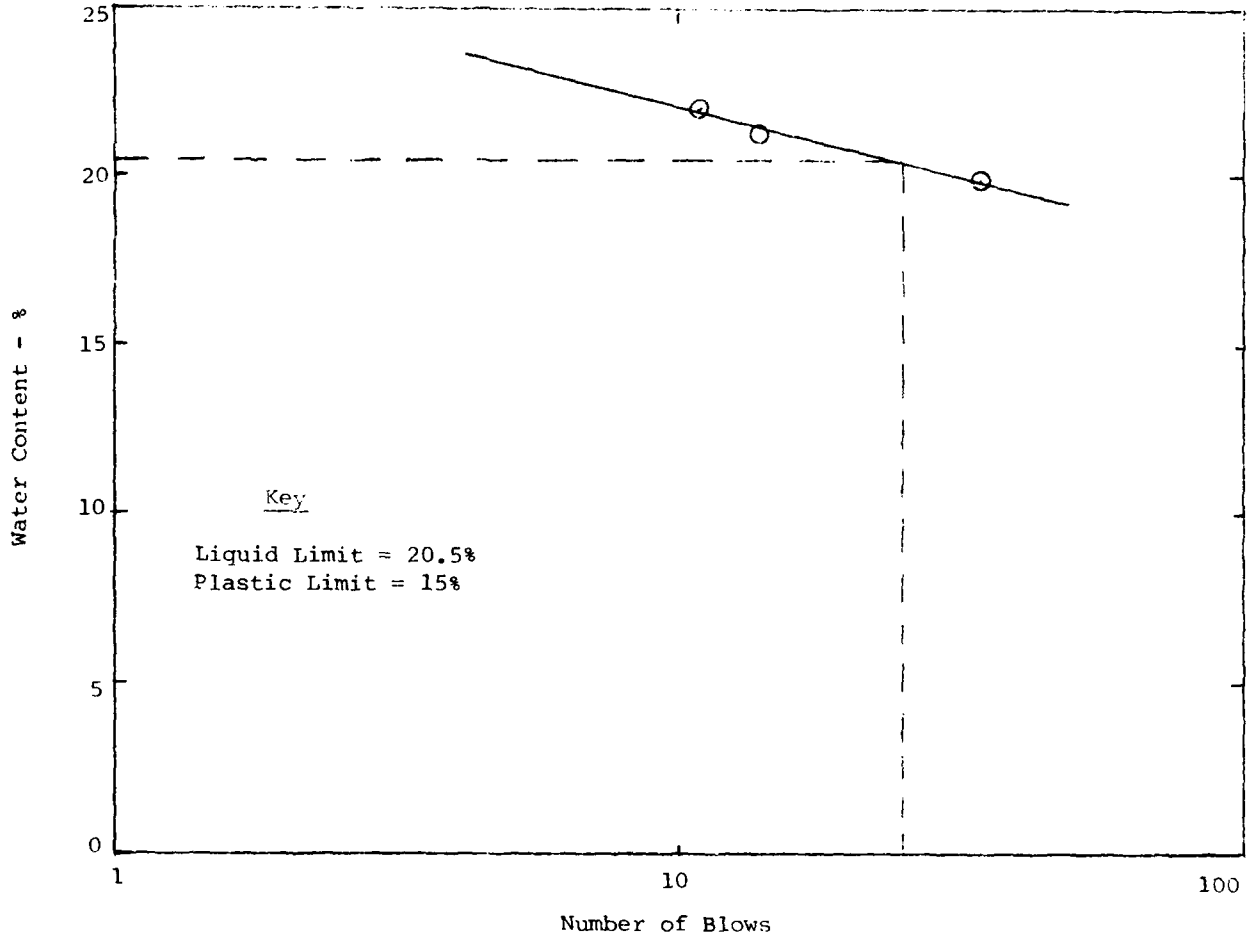

Fig. 3 The Liquid Limit on the Portion of Crushed Limestone Passing Thru the No. 200 Sieve.

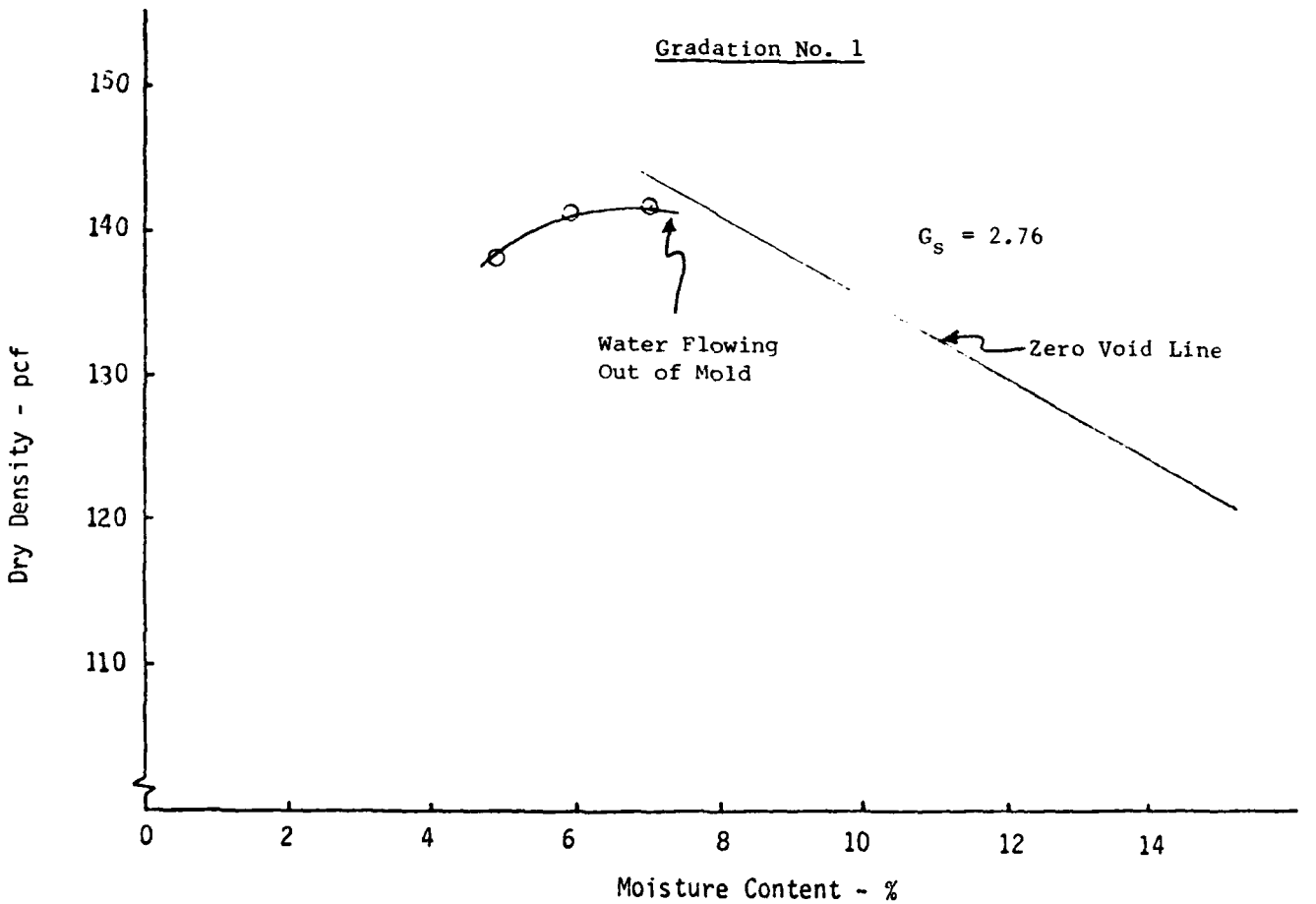

Fig. 4 CE-55 Impact Compaction Test Results for Gradation No. 1.

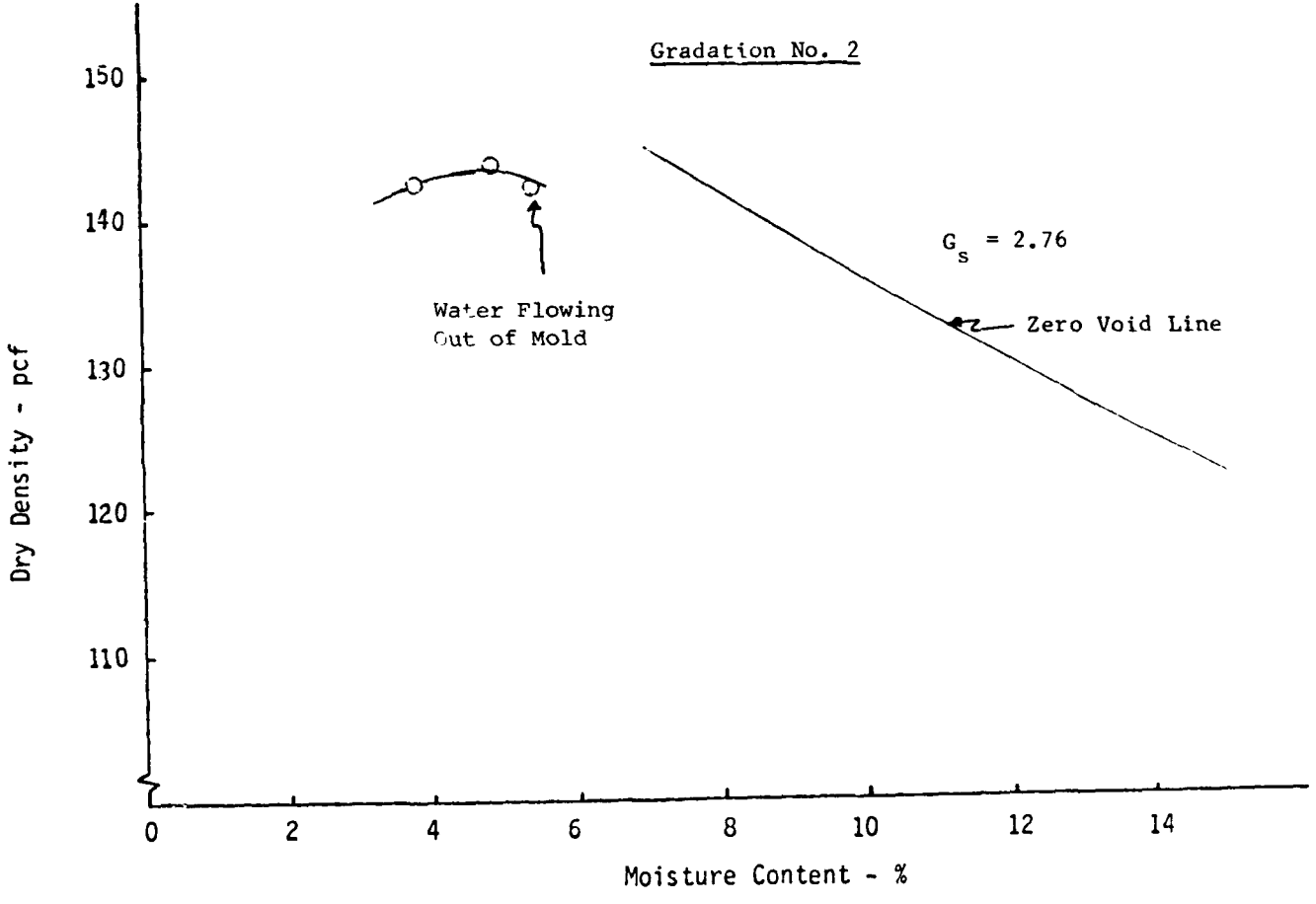

Fig. 5 CE-55 Impact Compaction Test Results for Gradation No 2.

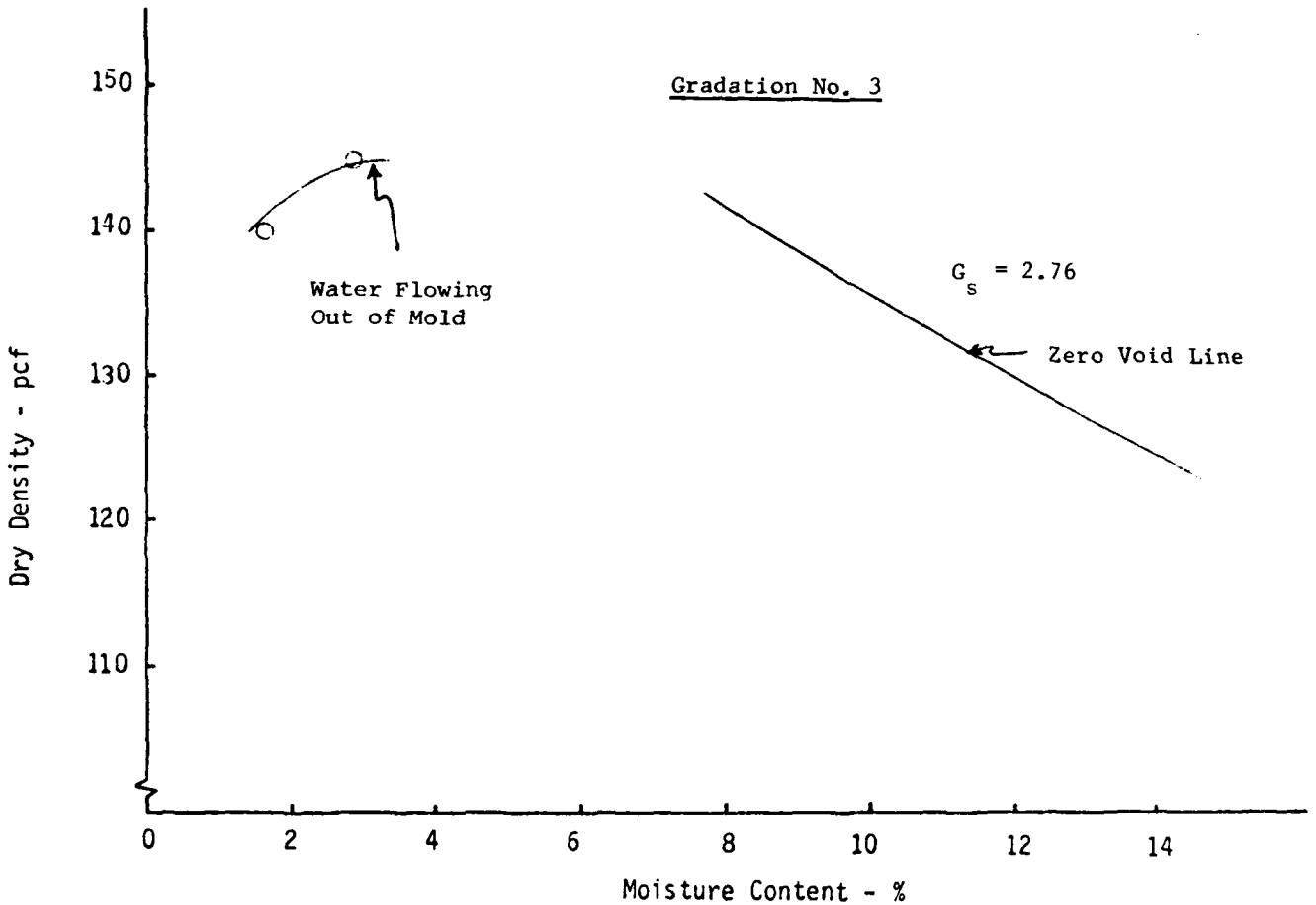

Fig. 6 CE-55 Impact Compaction Test Results for Gradation No. 3.

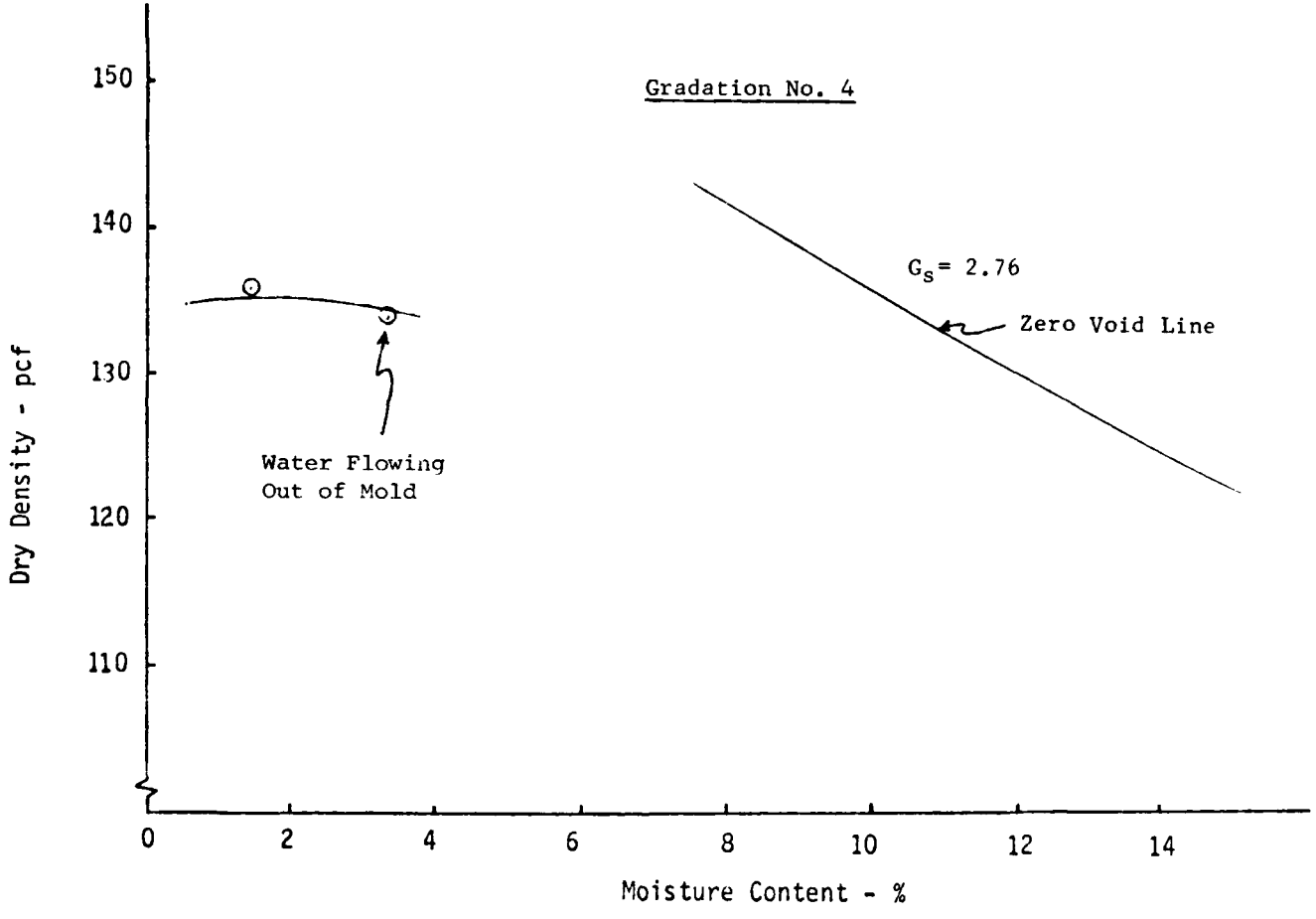

Fig. 7 CE-55 Impact Compaction Test Results for Gradation No. 4.

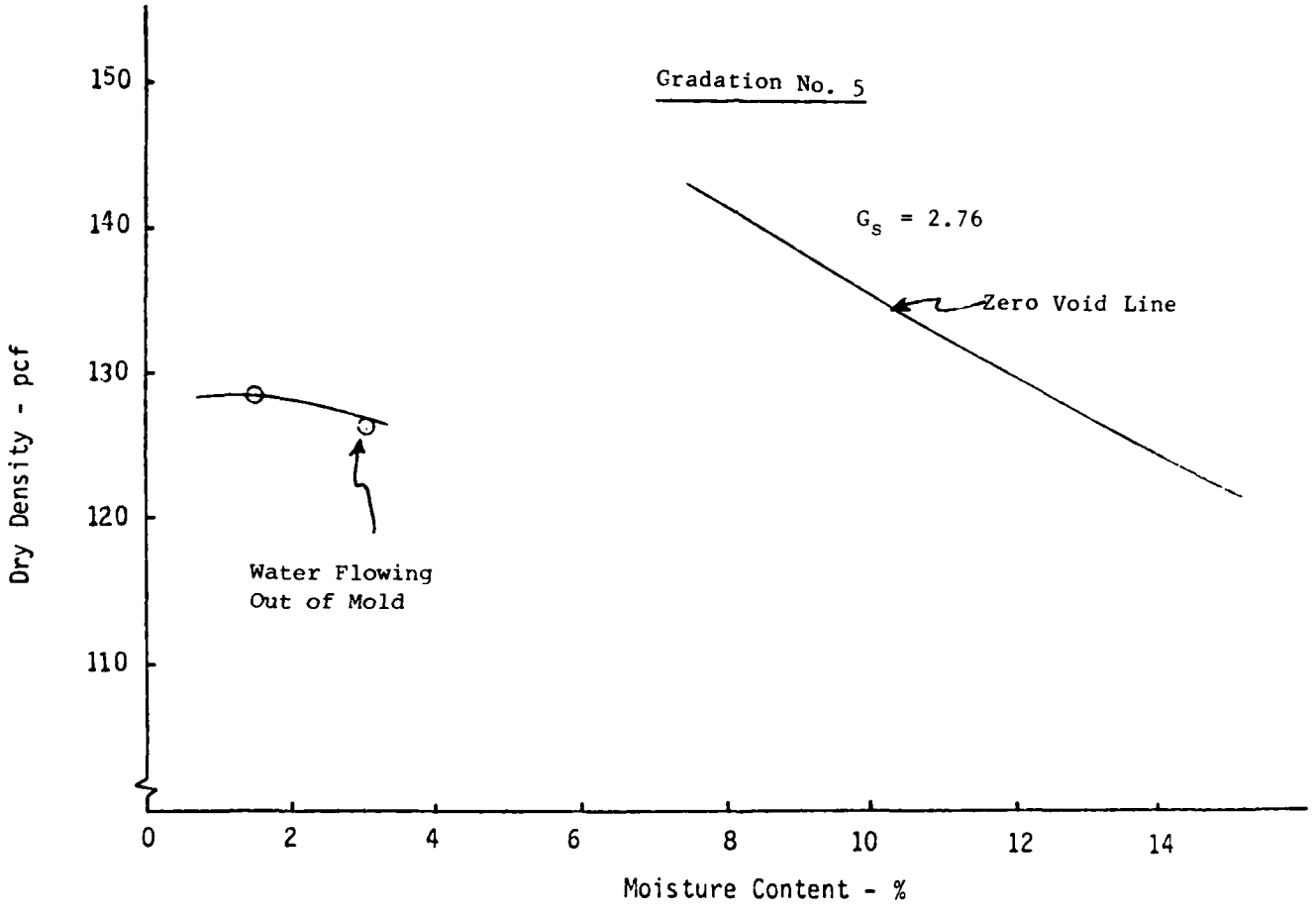

Fig. 8 CE-55 Impact Compaction Test Results for Gradation No. 5.

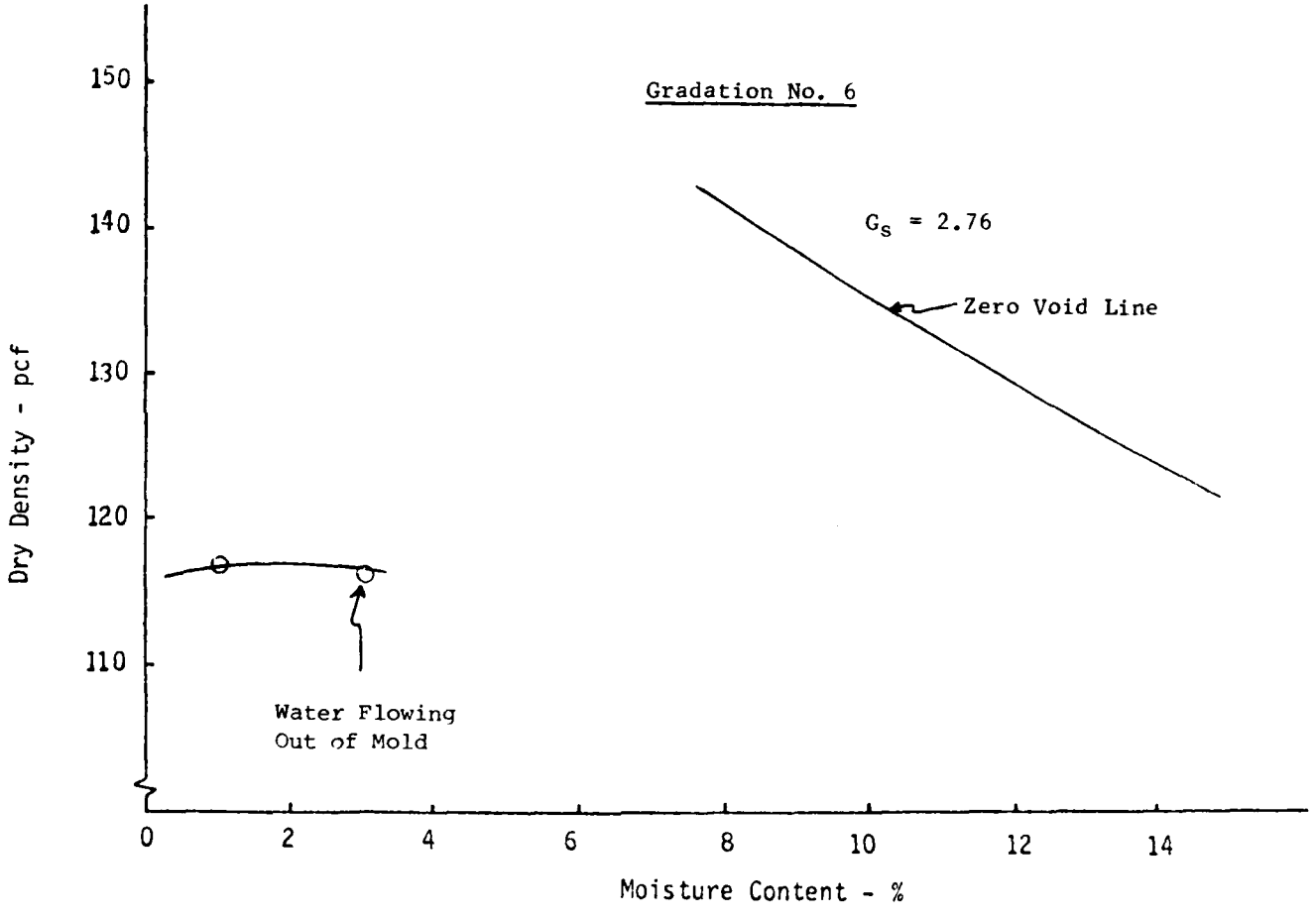

Fig. 9 CE-55 Impact Compaction Test Results for Gradation No. 6.

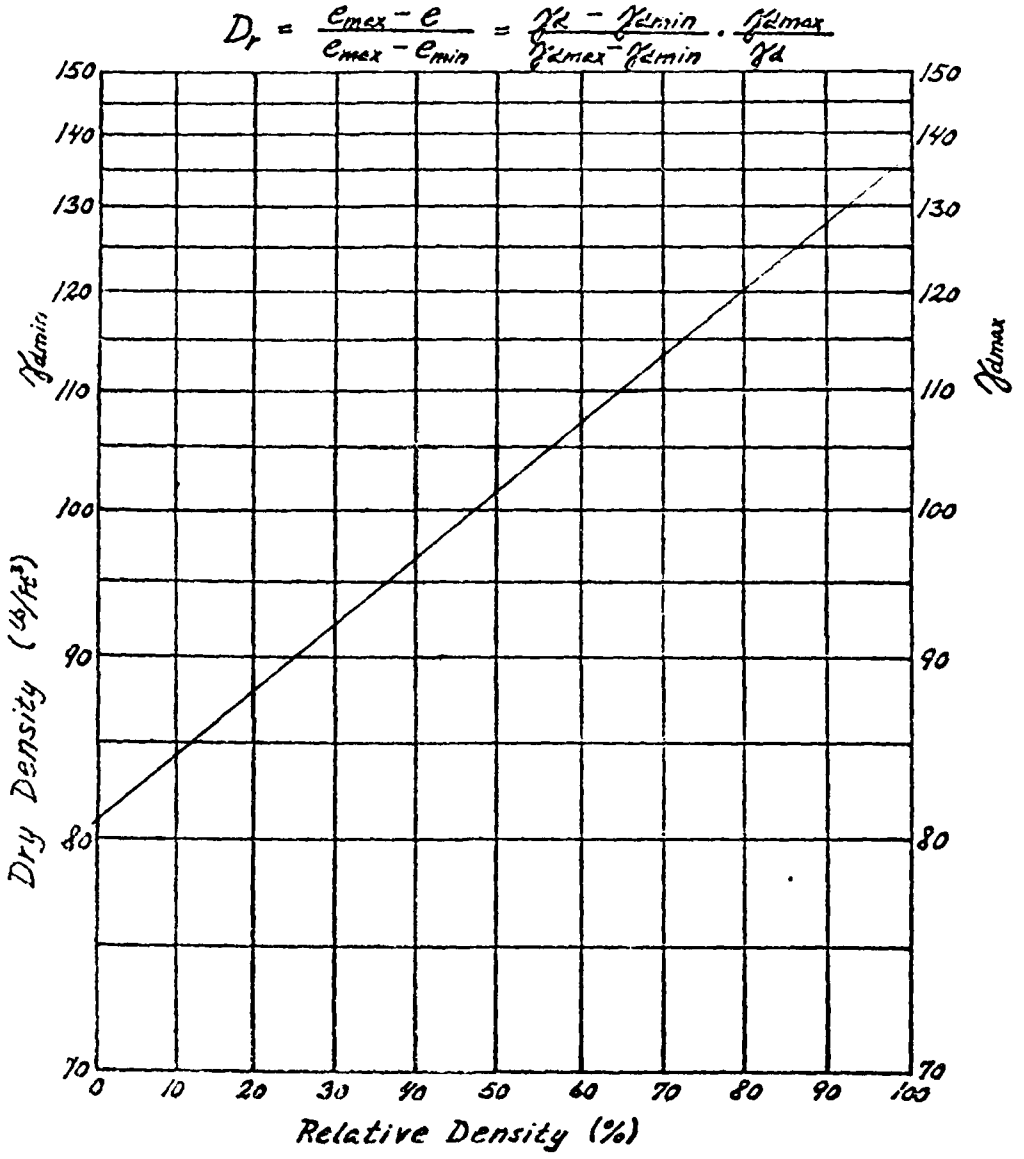

Fig. 10 Diagram for Relation Between Relative Density and Dry Density (scaled to plot as a straight line). γ_d max is based on Modified Proctor Density

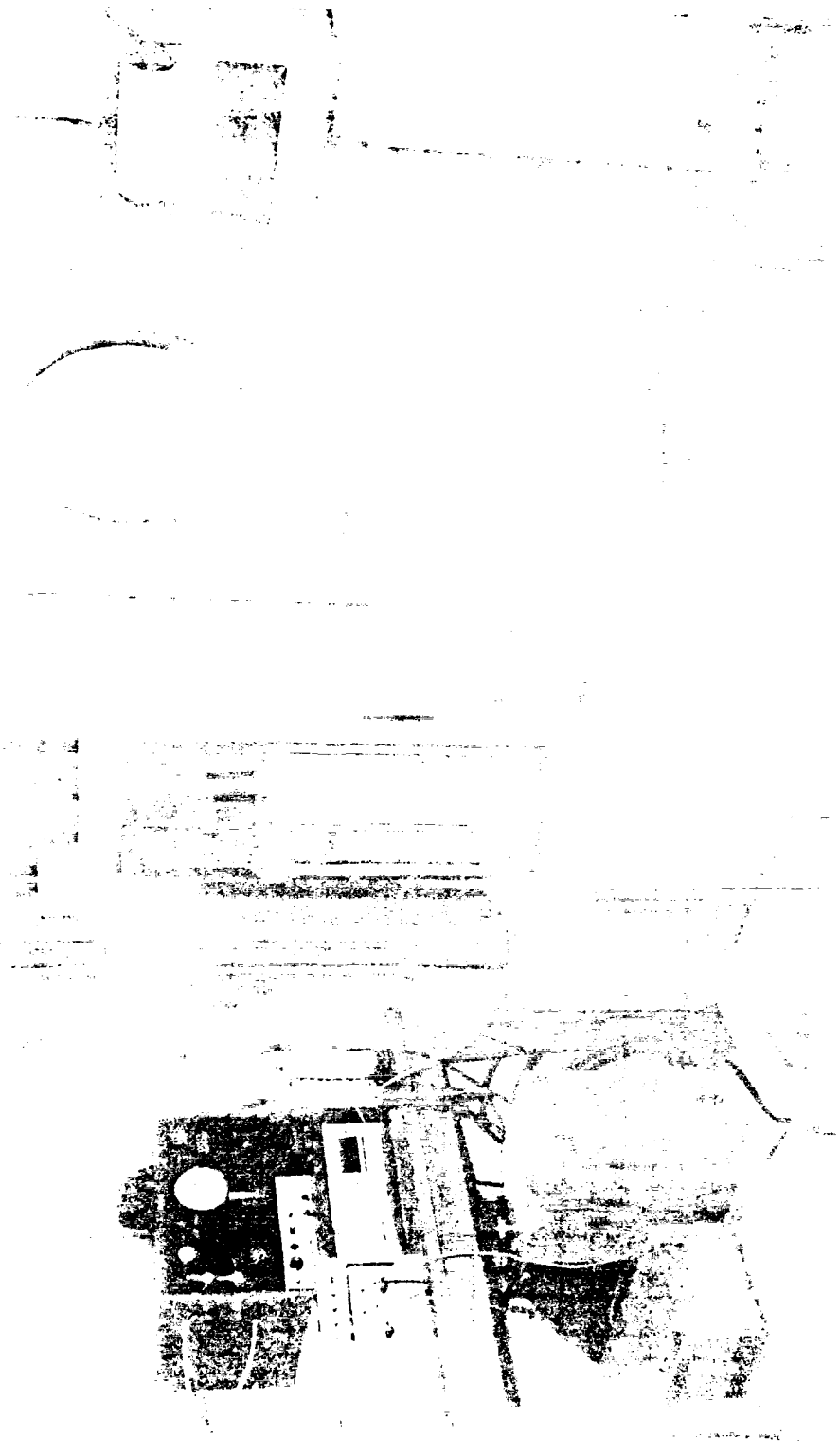

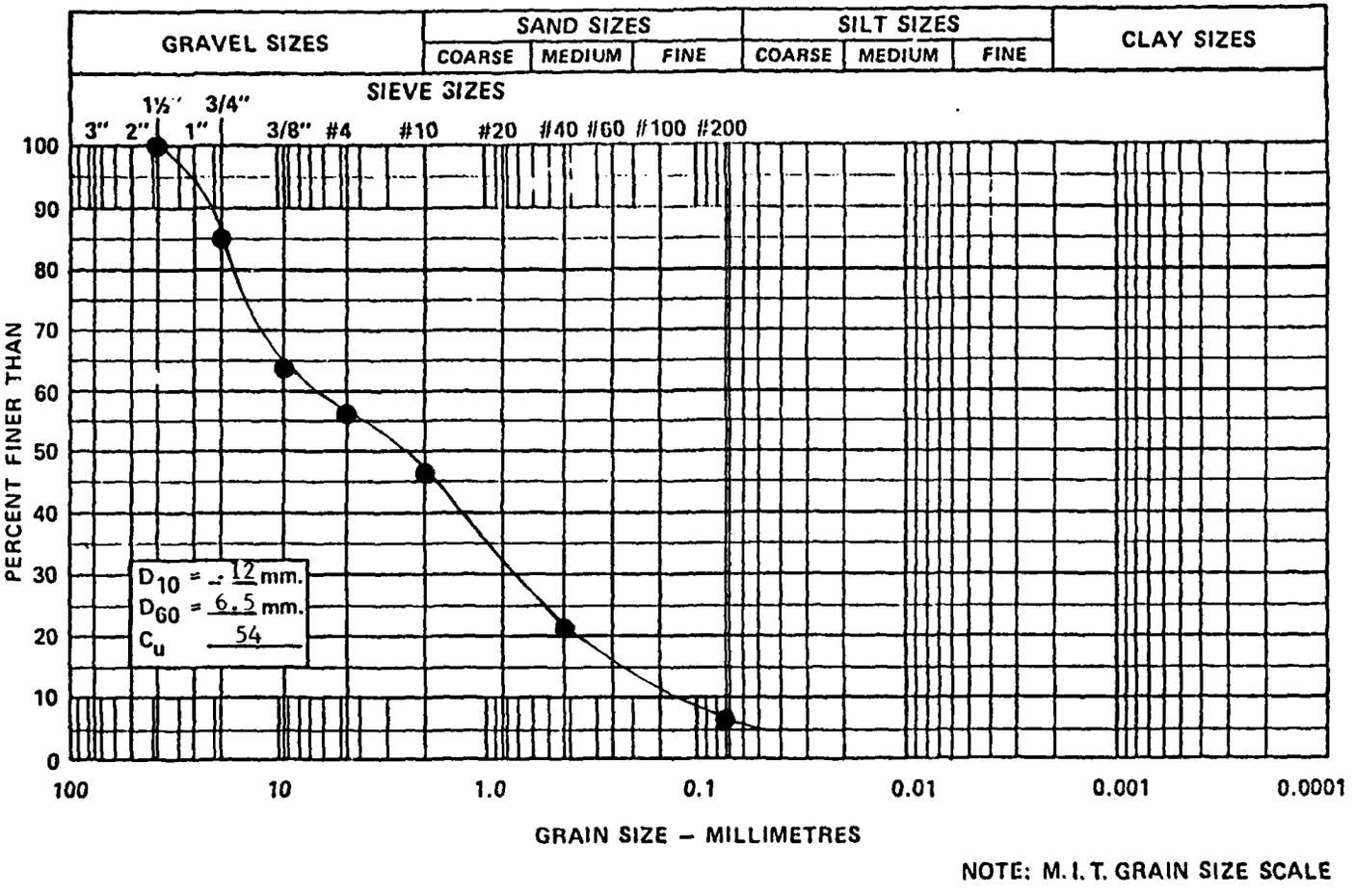

Fig. 12 GRAIN SIZE DISTRIBUTION CURVE FOR GRADATION NO. 1, Series A.

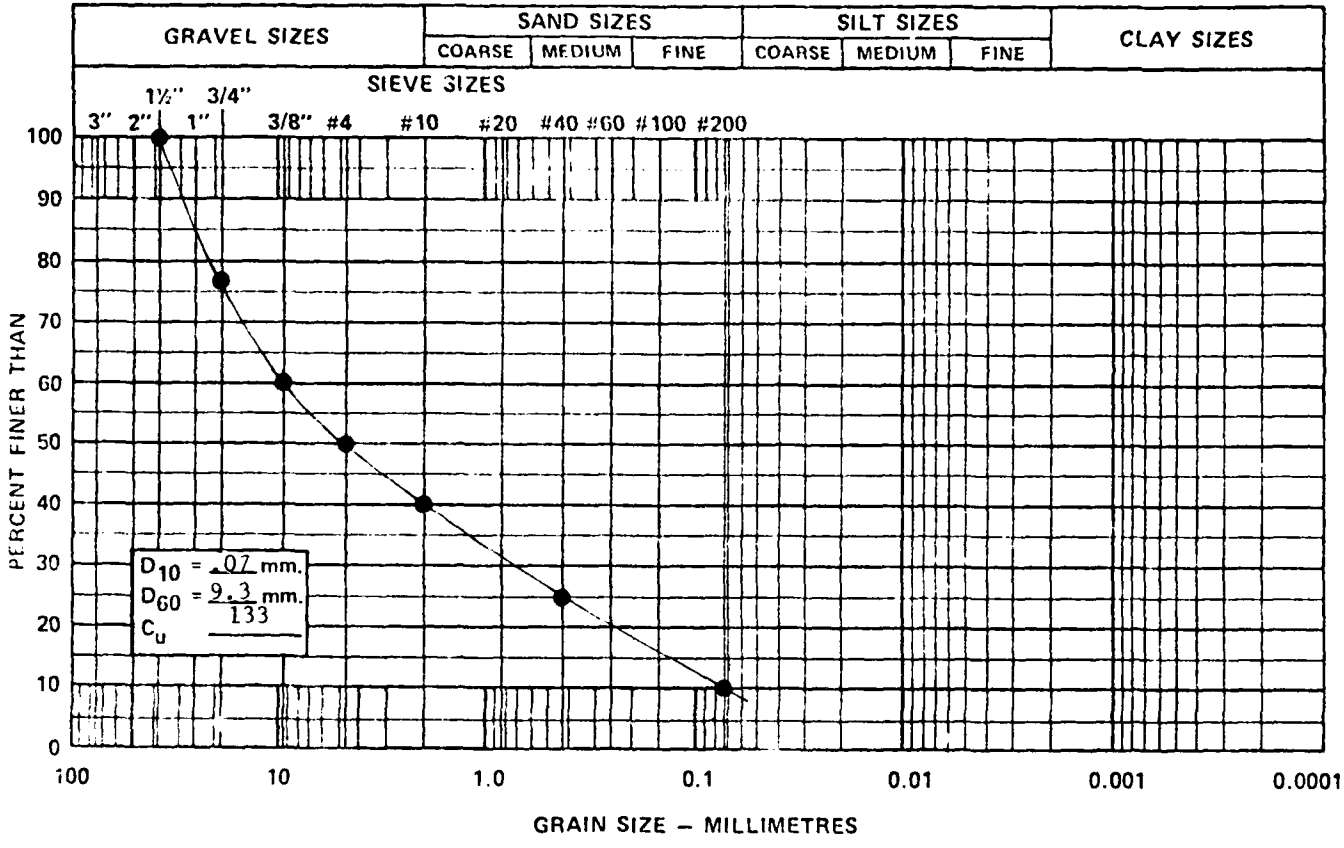

Fig. 13 GRAIN SIZE DISTRIBUTION CURVE FOR GRADATION NO. 2, Series B.

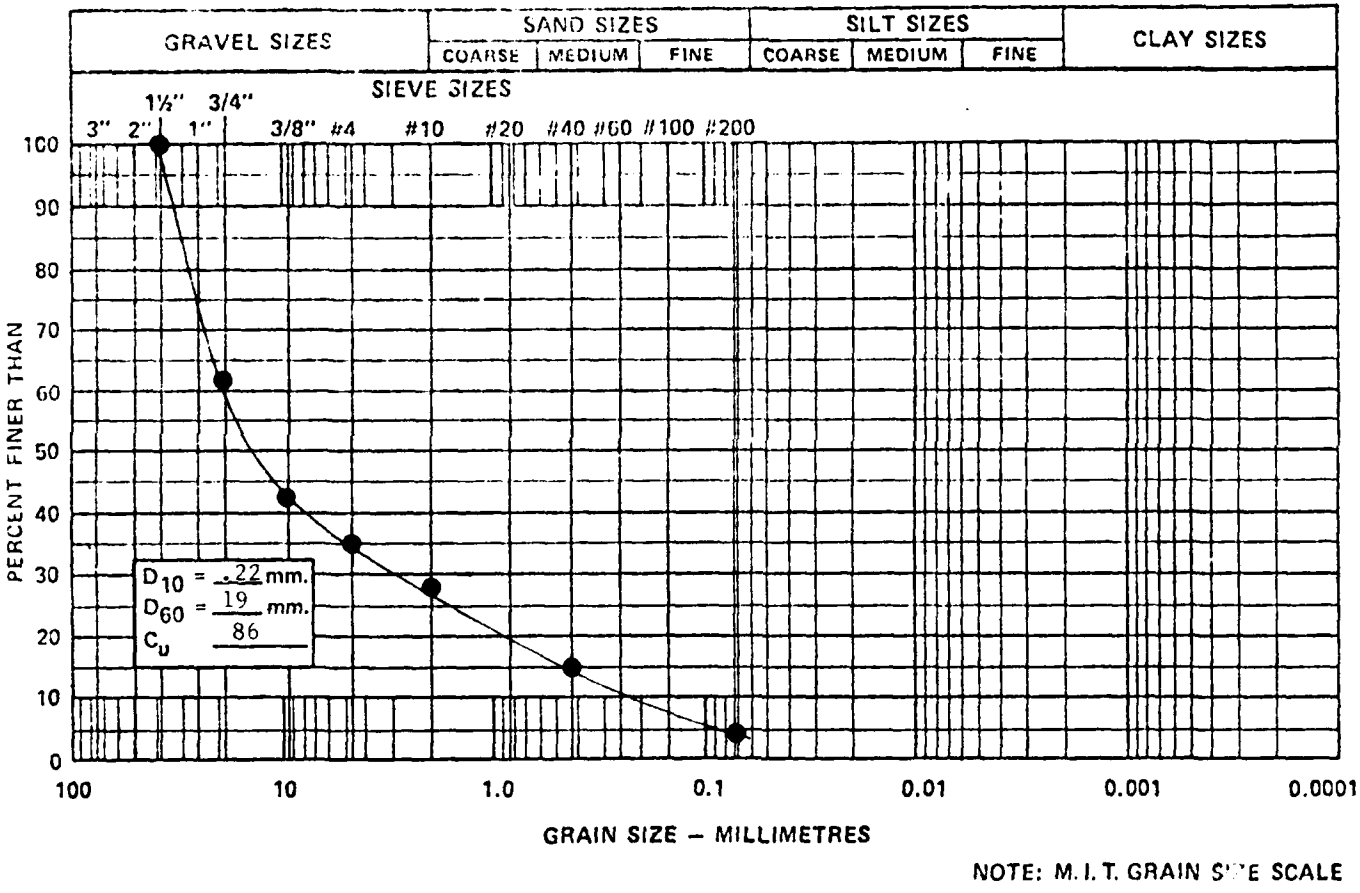

Fig. 14 **GRAIN SIZE DISTRIBUTION CURVE FOR** GRADATION NO. 3, Series C.

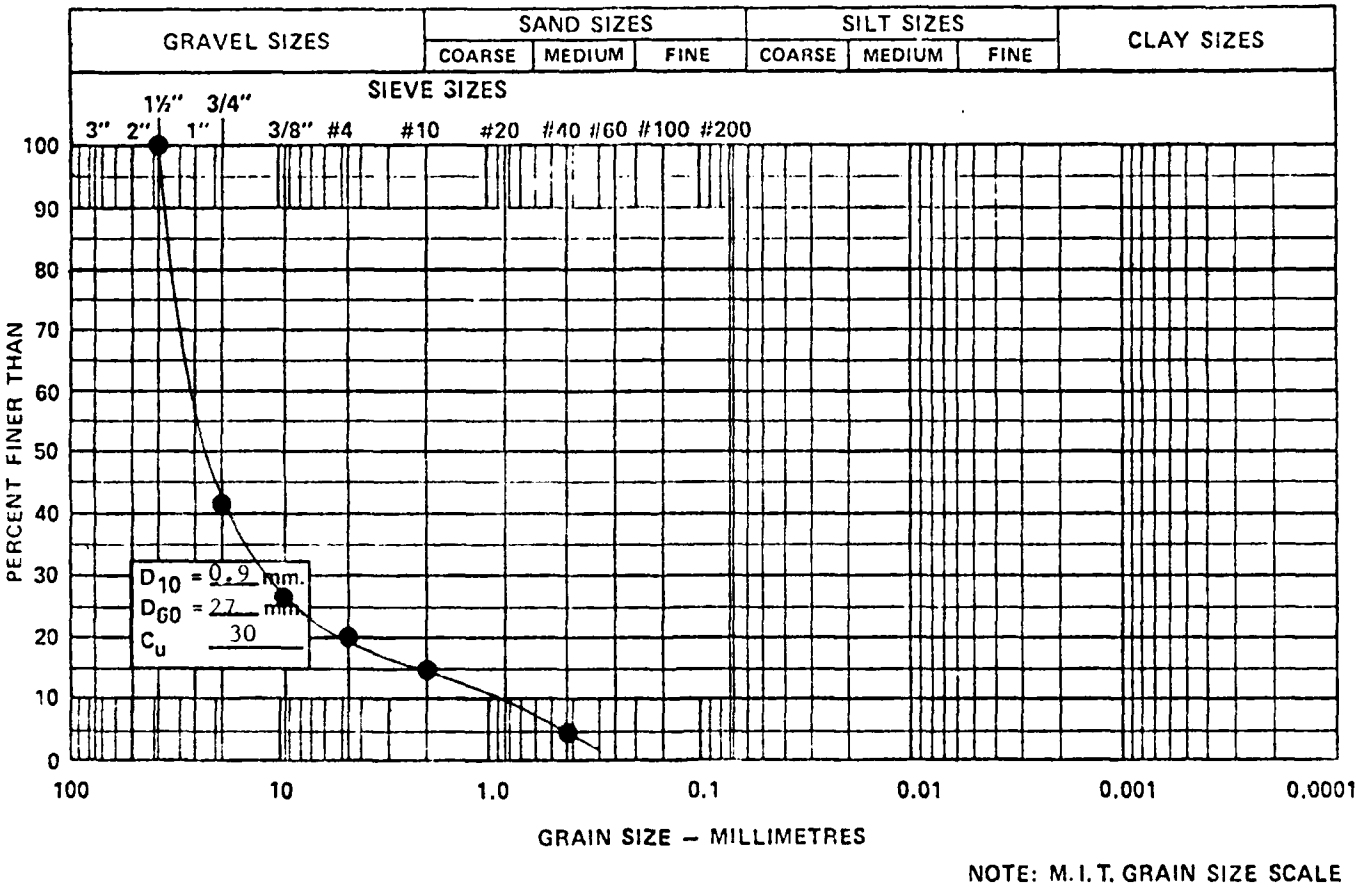

Fig. 15 GRAIN SIZE DISTRIBUTION CURVE FOR GRADATION NO. 4, Series D.

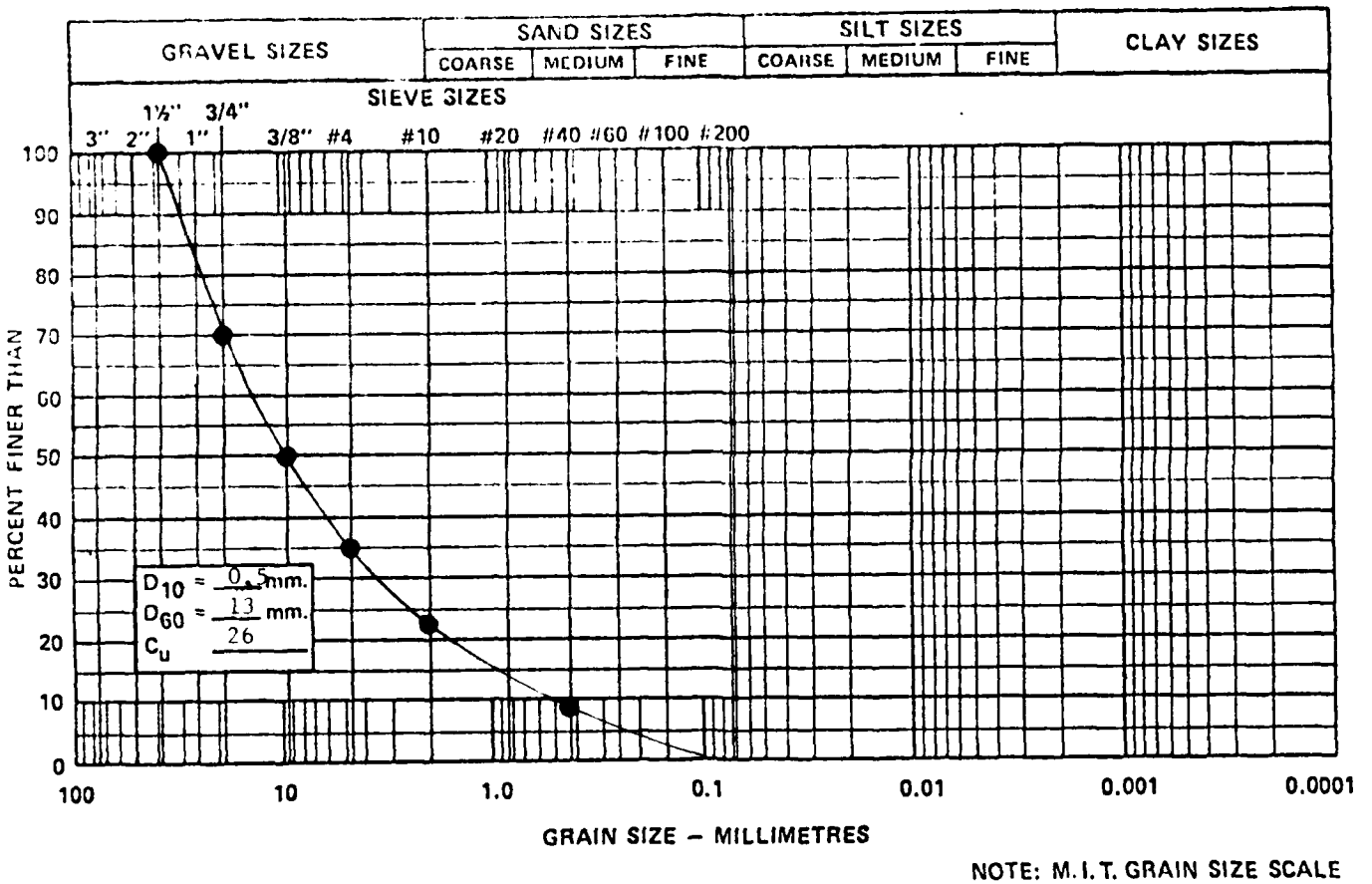

Fig. 1e GRAIN SIZE DISTRIBUTION CURVE FOR GRADATION 5, Series E.

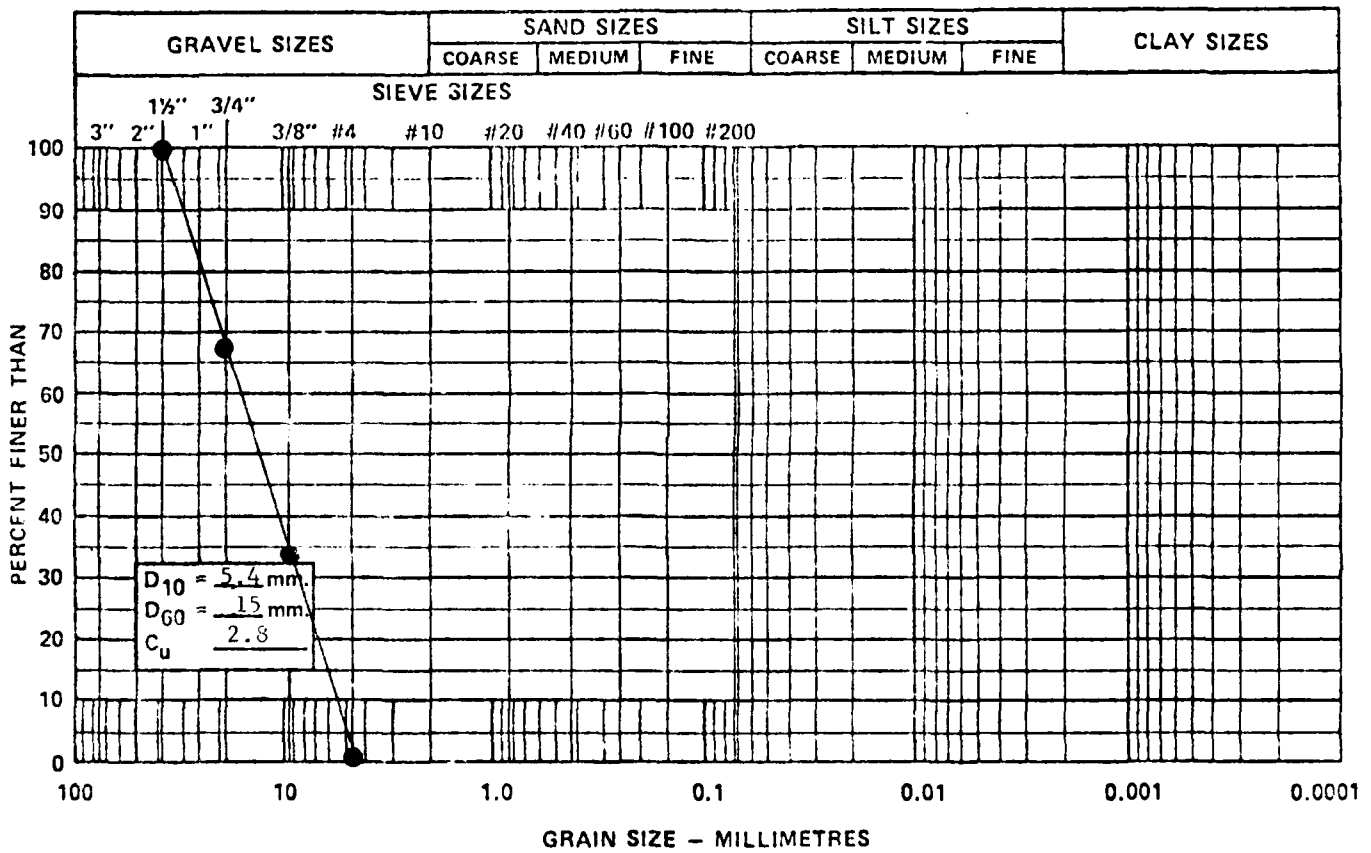

Fig. 17 **GRAIN SIZE DISTRIBUTION CURVE FOR** GRADATION NO. 6, Series F.

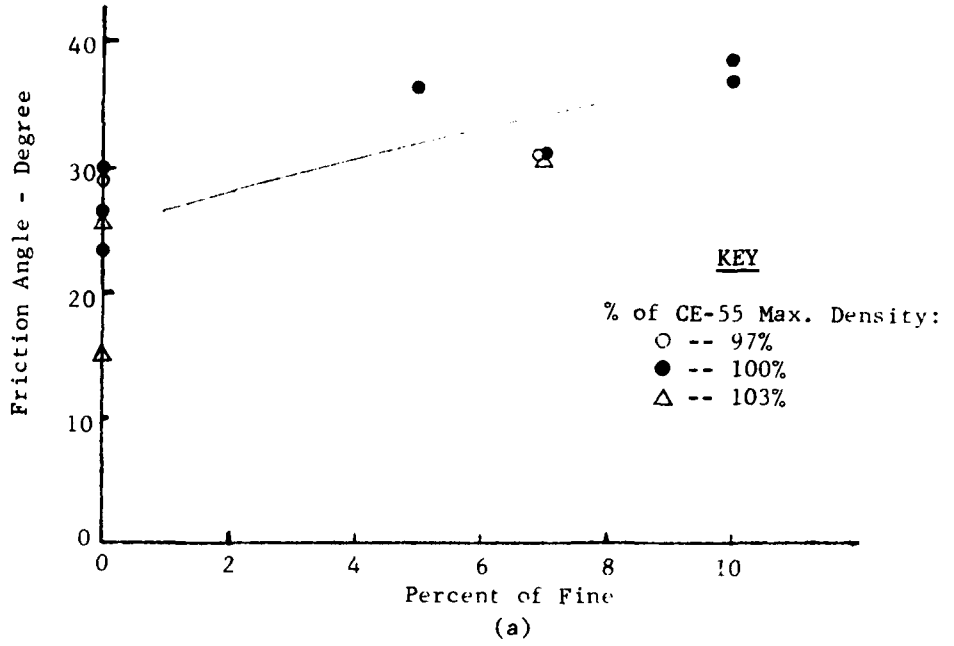

(a)

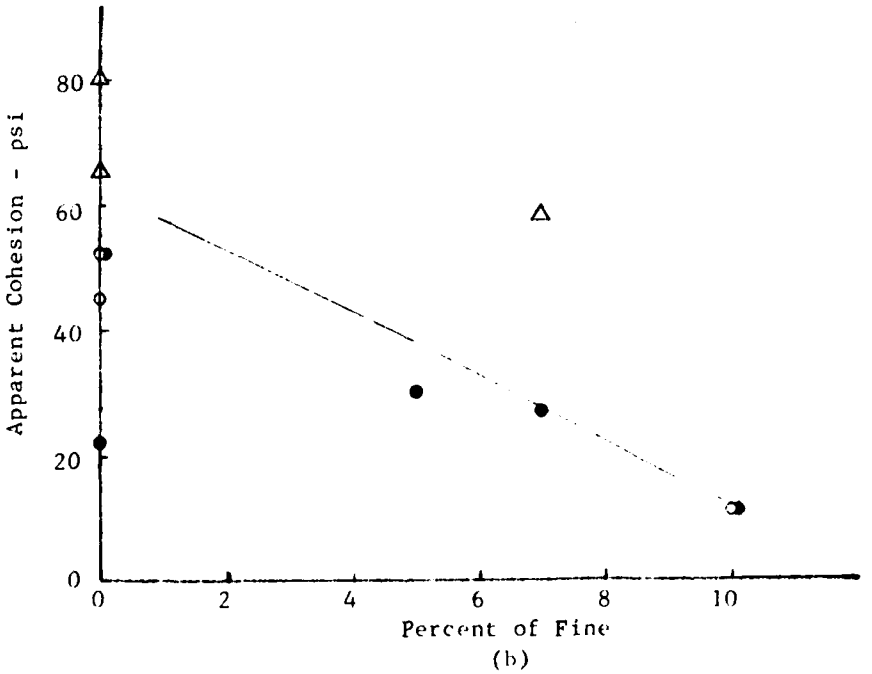

(b)

Fig. 18 The Effects of Fine on the Friction Angle and the Apparent Cohesion for all gradations.

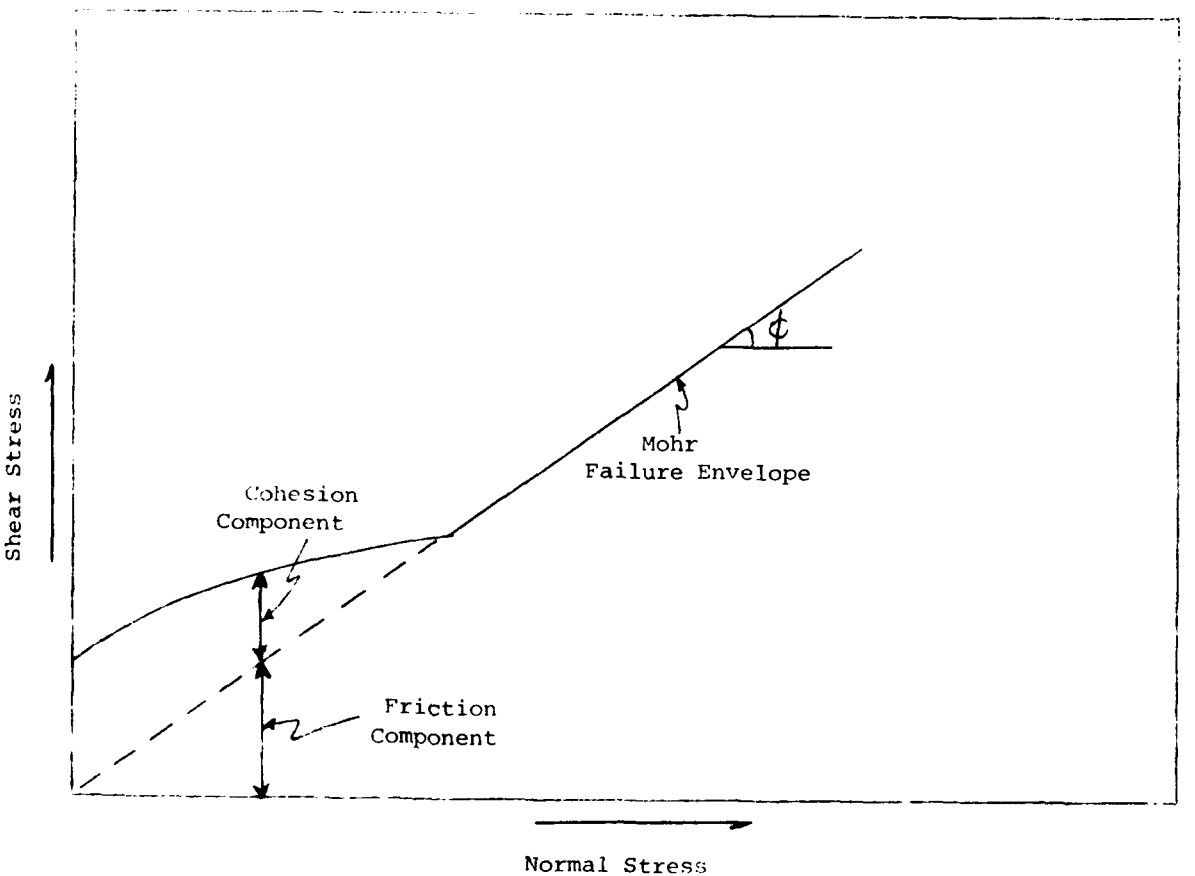

Fig.19 The Effect of the Cohesion Component on the Mohr Envelope at Low Confining Stresses.

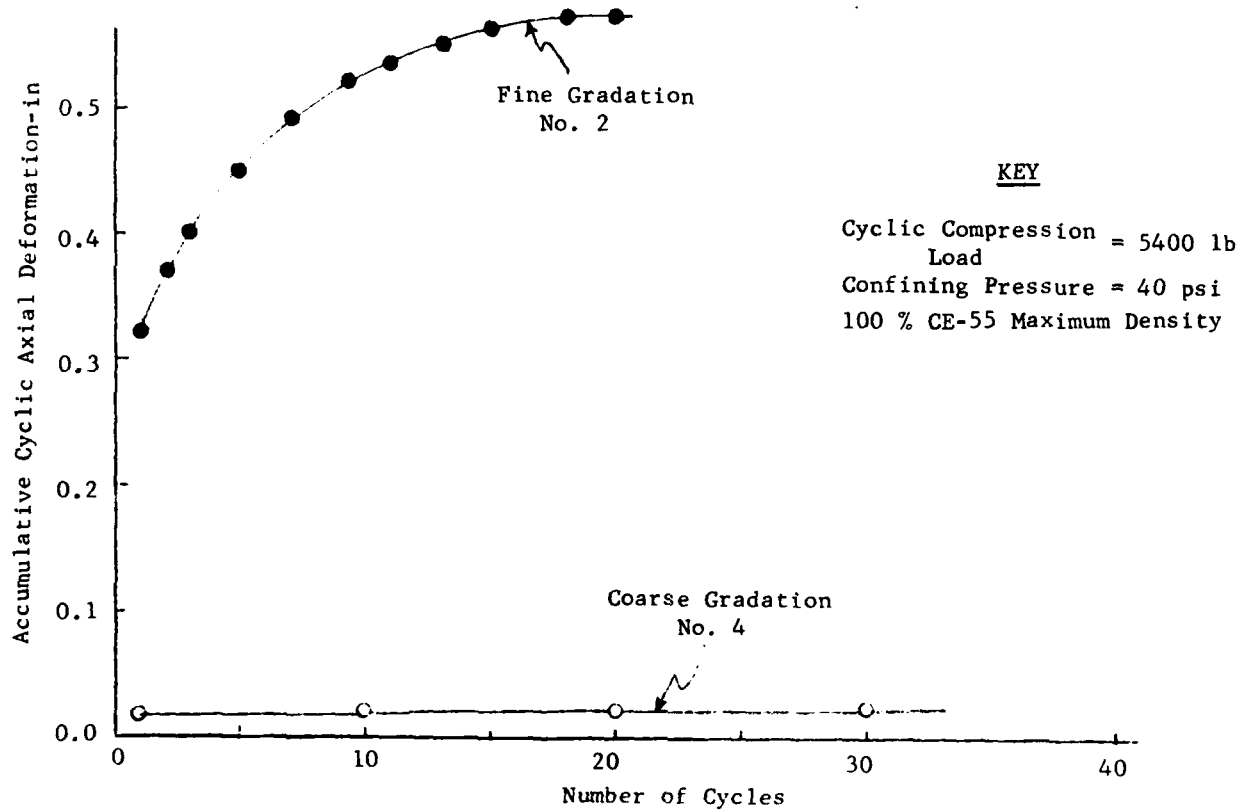

Fig. 20 Comparison of Accumulative Cyclic Axial Deformation Between Fine and Coarse Gradations.

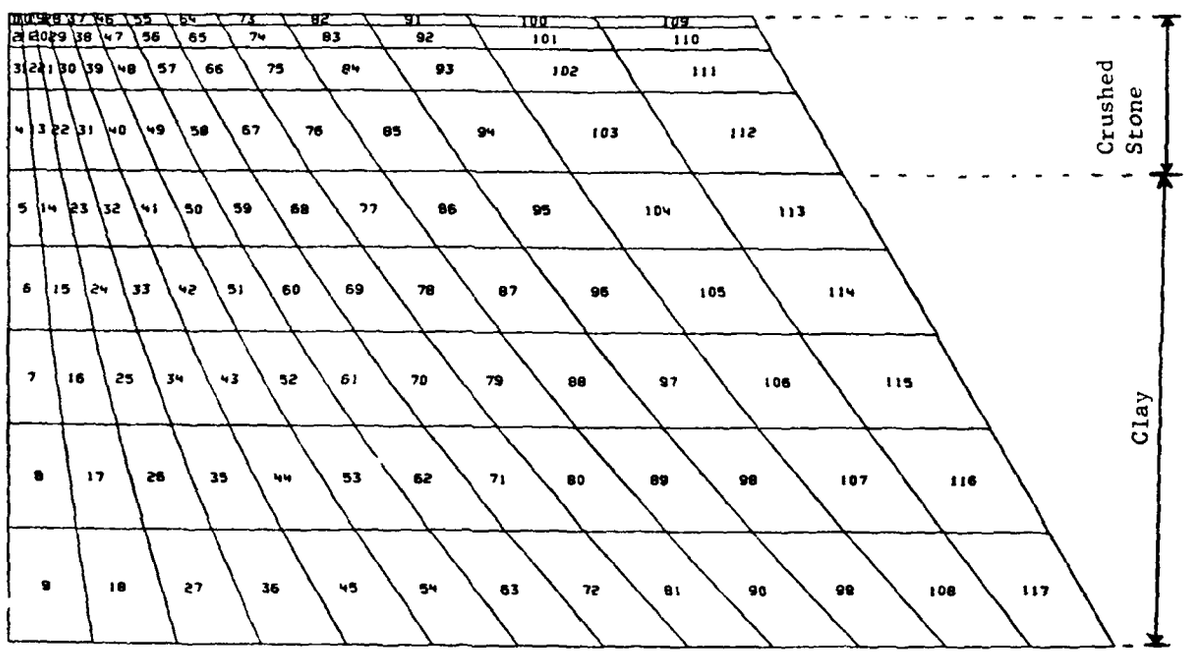

Fig. 21 The Element Numbers of the Computer Model.

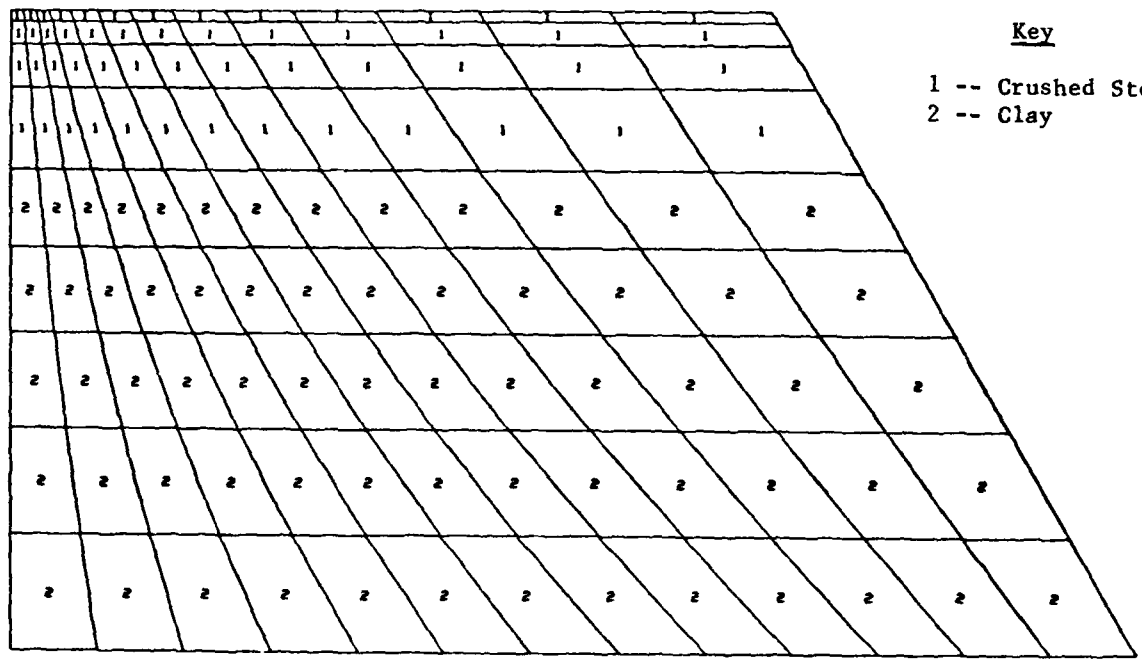

Fig. 22 Materials of the Computer Model.

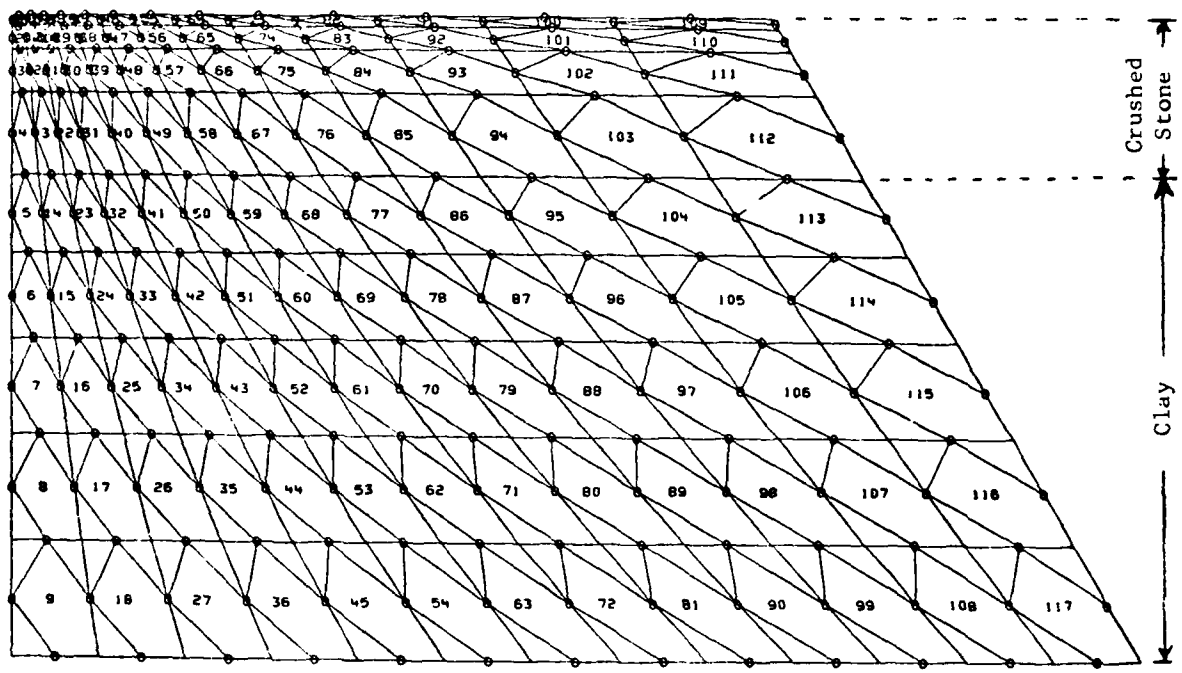

Fig. 23 Finite Element Mesh Showing Midside Node Display.

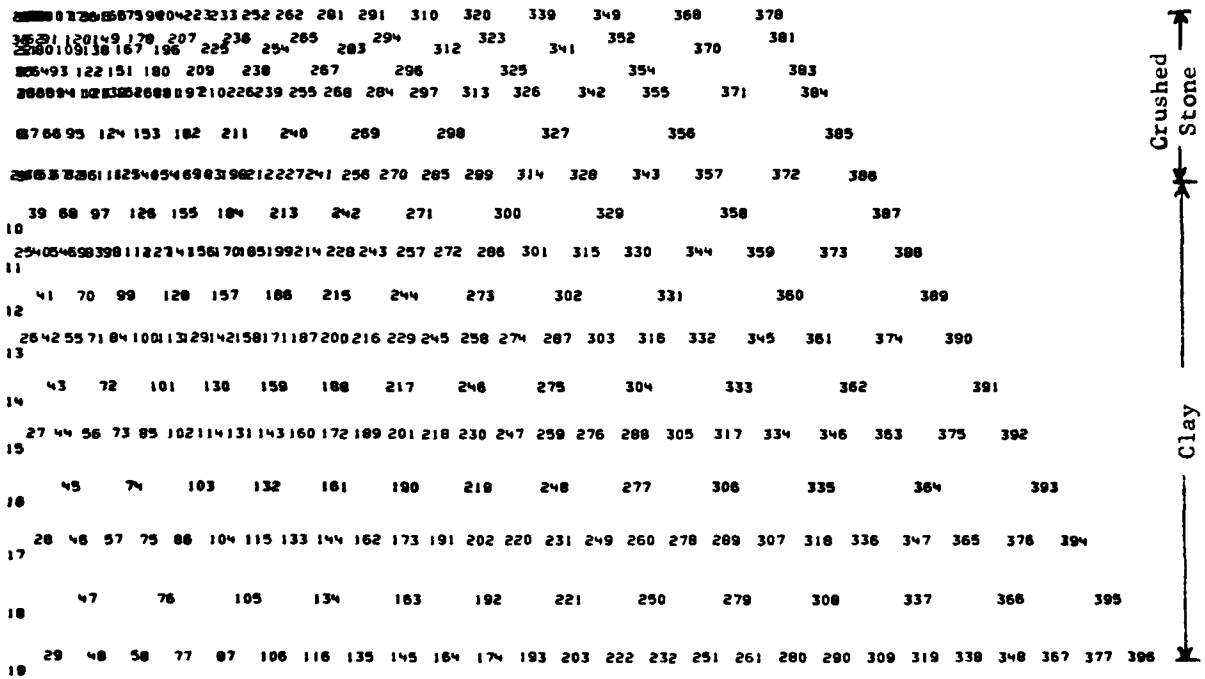

Fig. 24 The Nodal Point Numbers of the Computer Model.

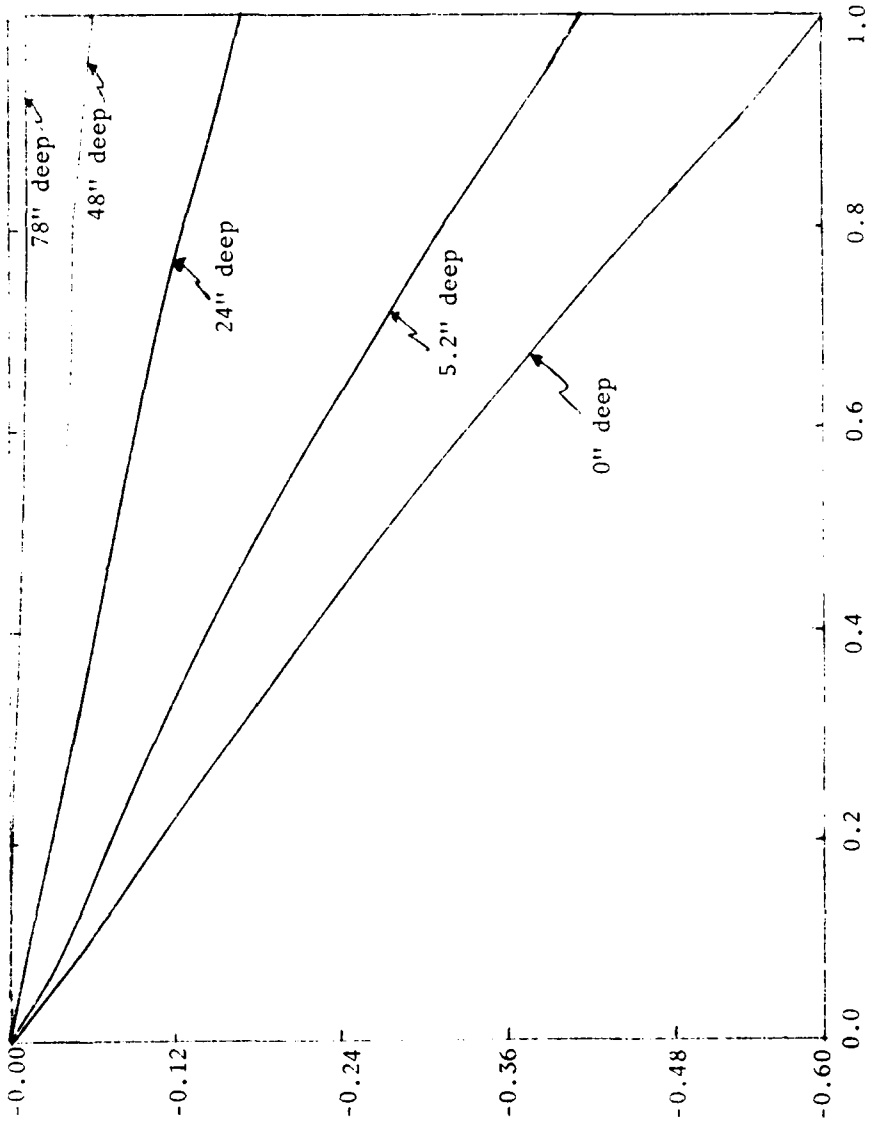

Fig. 25 The Relationship of Vertical Displacement Along the Centerline of Wheel Load Versus Depth and Fraction of Wheel Load for Soil Model No. 5.

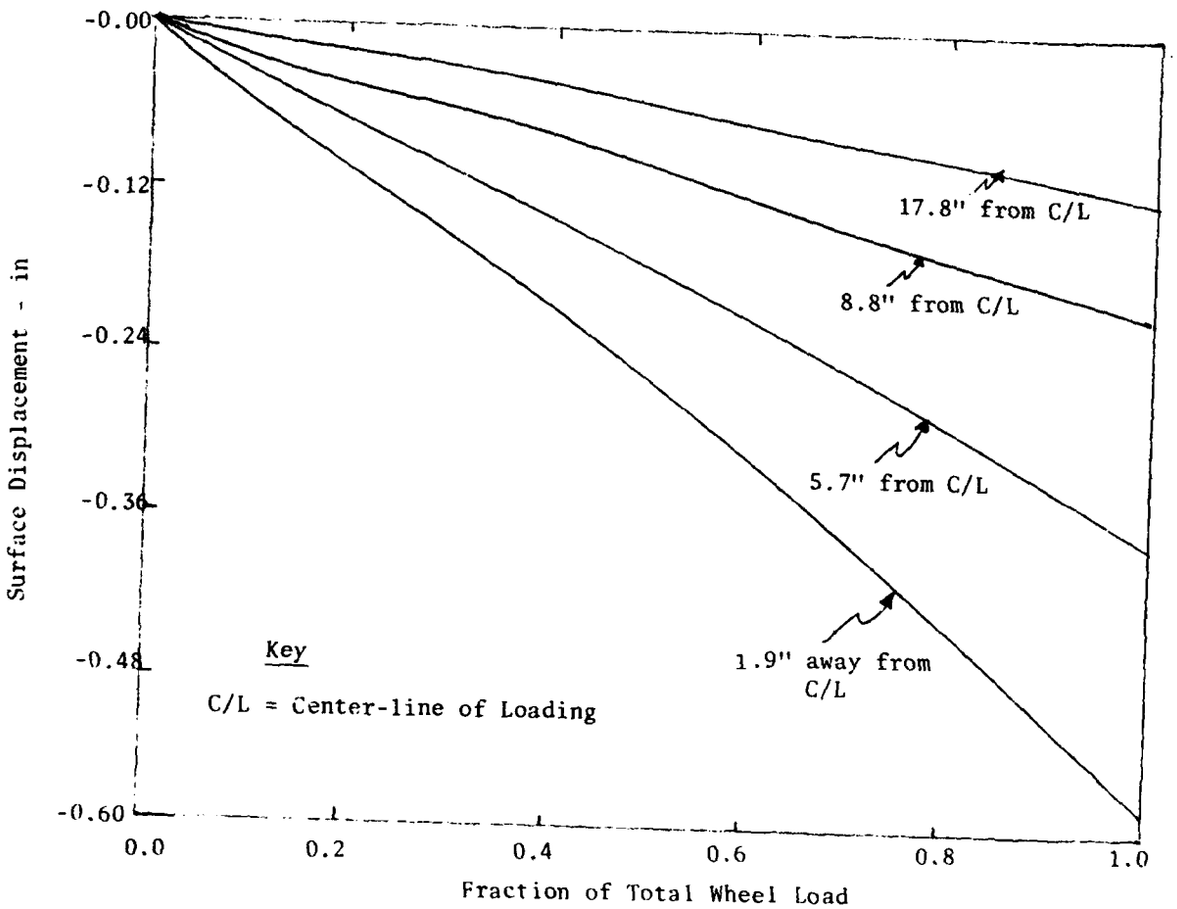

Fig. 26 The Relationship of Vertical Displacement along the Surface Versus Distance Away from the Center-line of loading and Fraction of Total Wheel Load for Soil Model No. 5.

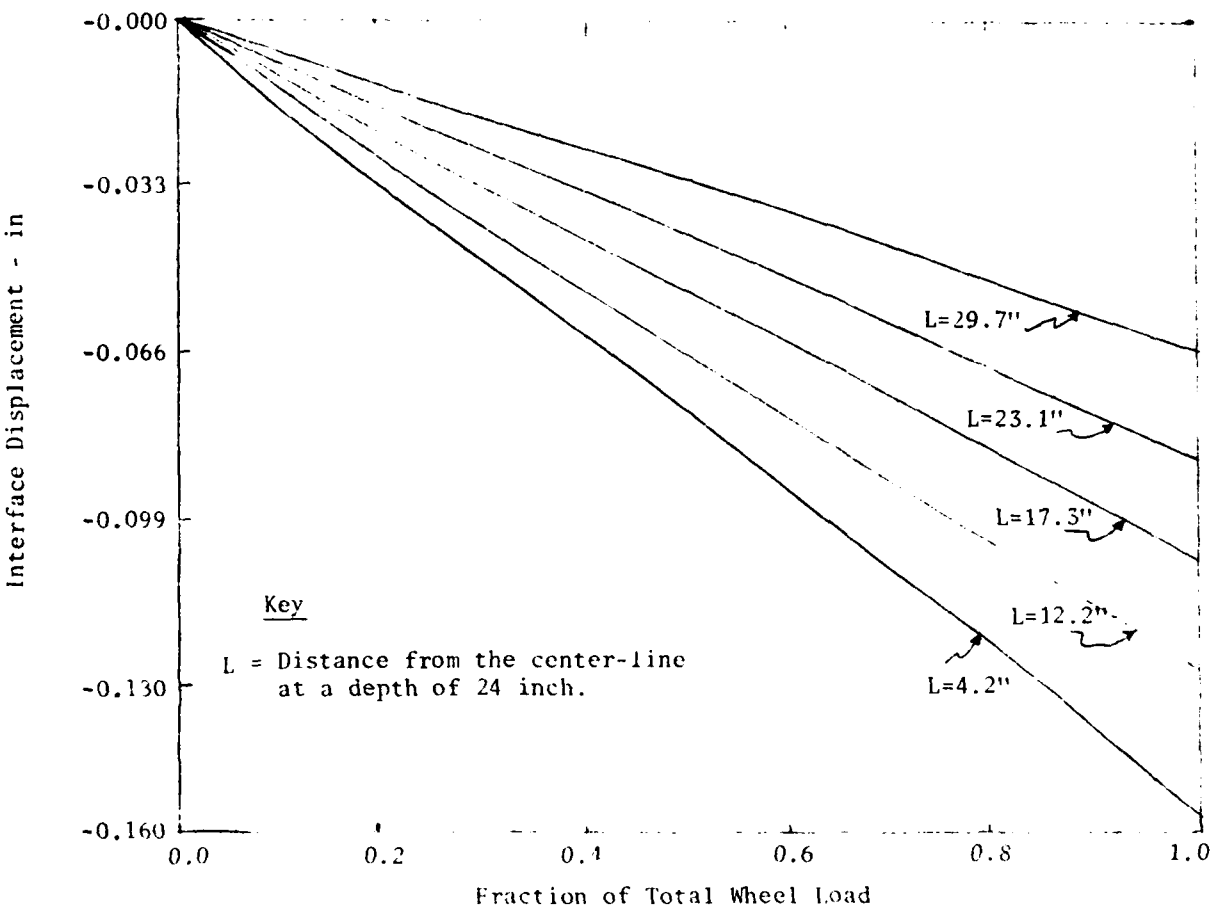

Fig. 27 The Relationship of Interface Displacement at a Depth of 24 inch. Versus Distance from the Center-line and Fraction of Total Wheel Load for Soil Model No. 5.

(The reverse of this page is blank)

Appendix

Original Triaxial Test Data

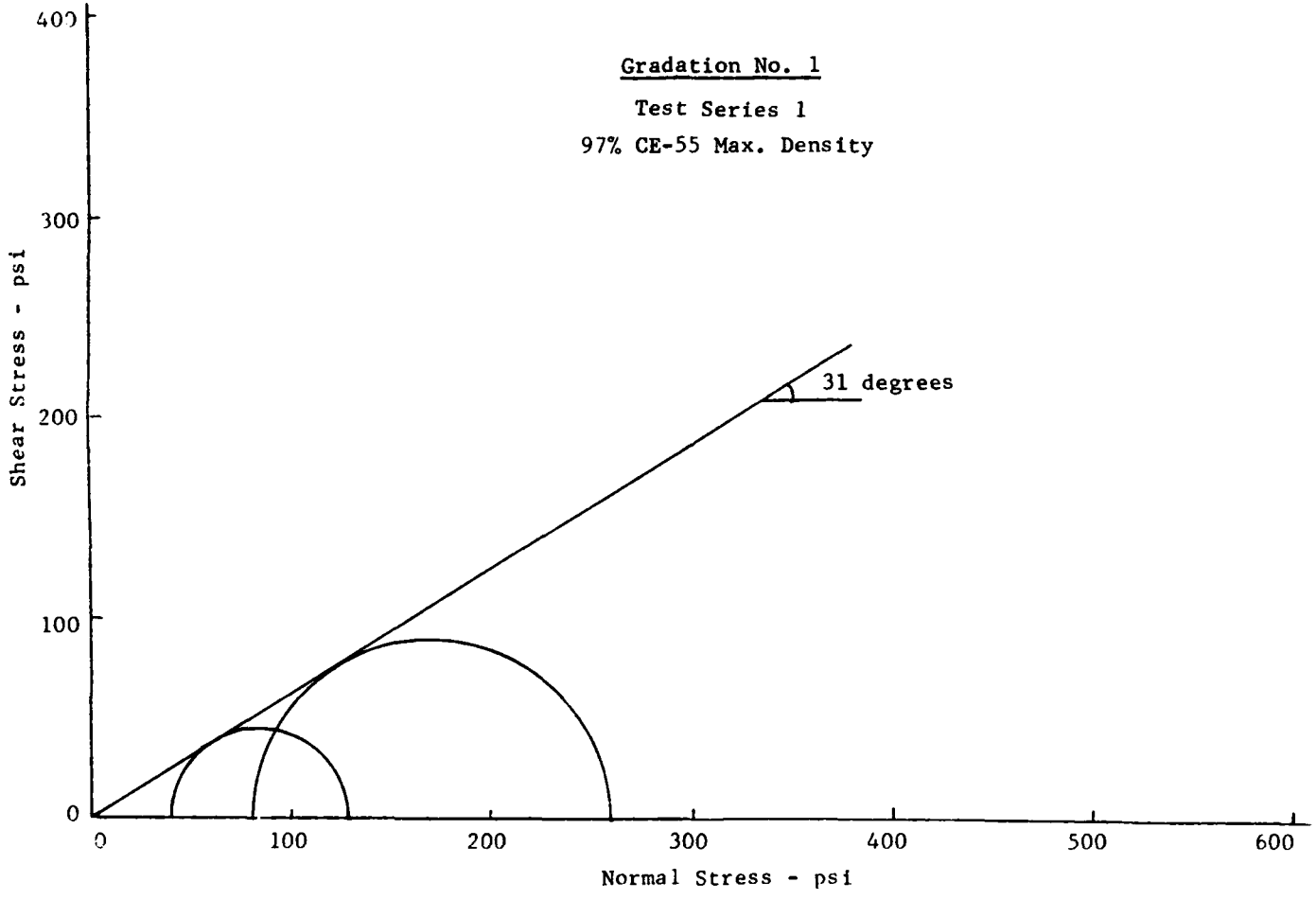

Fig. A-1 Mohr Failure Envelope For Gradation No. 1, 97 % Max. Density.

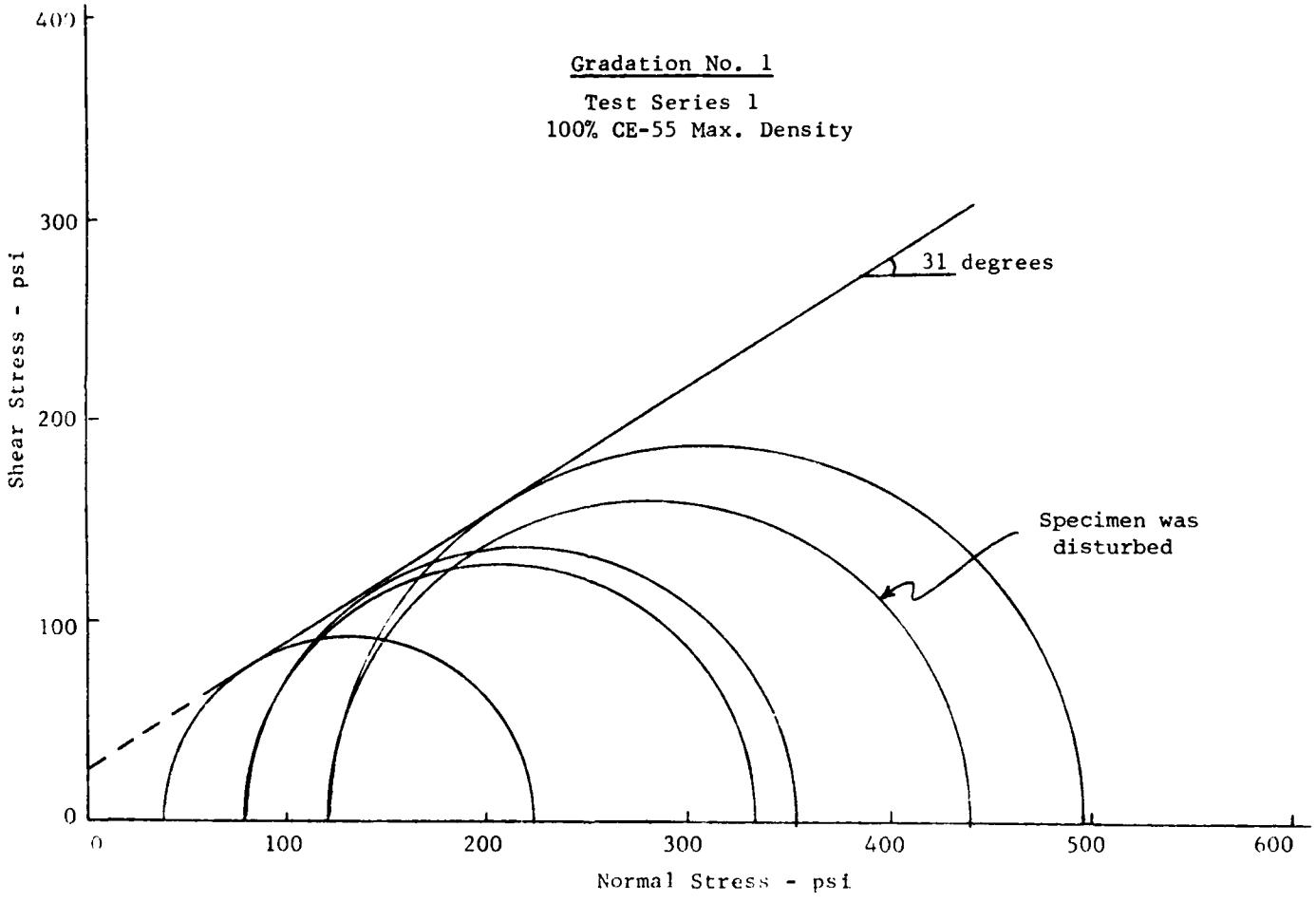

Fig. A-2 Mohr Failure Envelope For Gradation No. 1, 100% Max. Density.

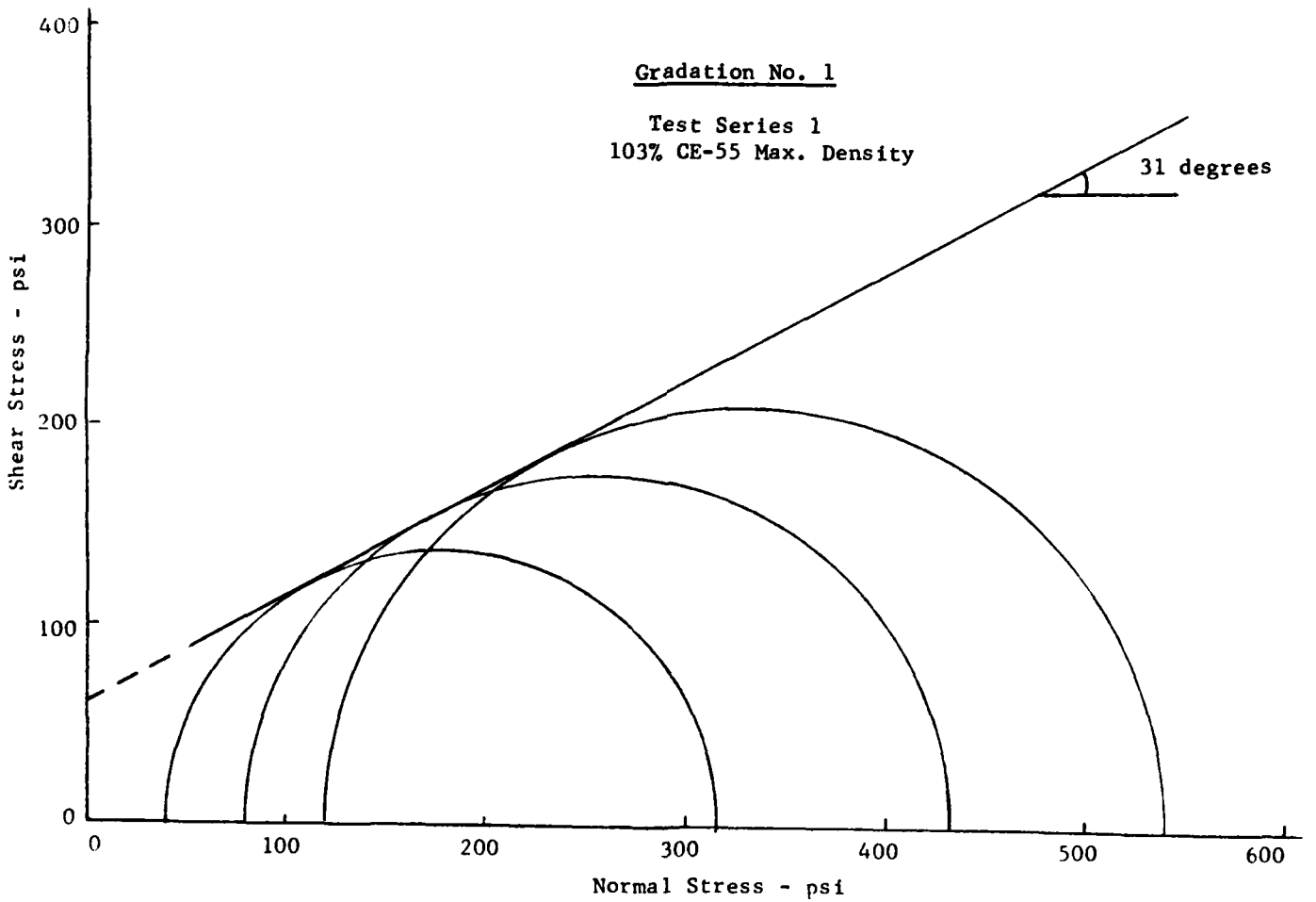

Fig. A-3 Mohr Failure Envelope for Gradation No. 1, 103% Max. Density.

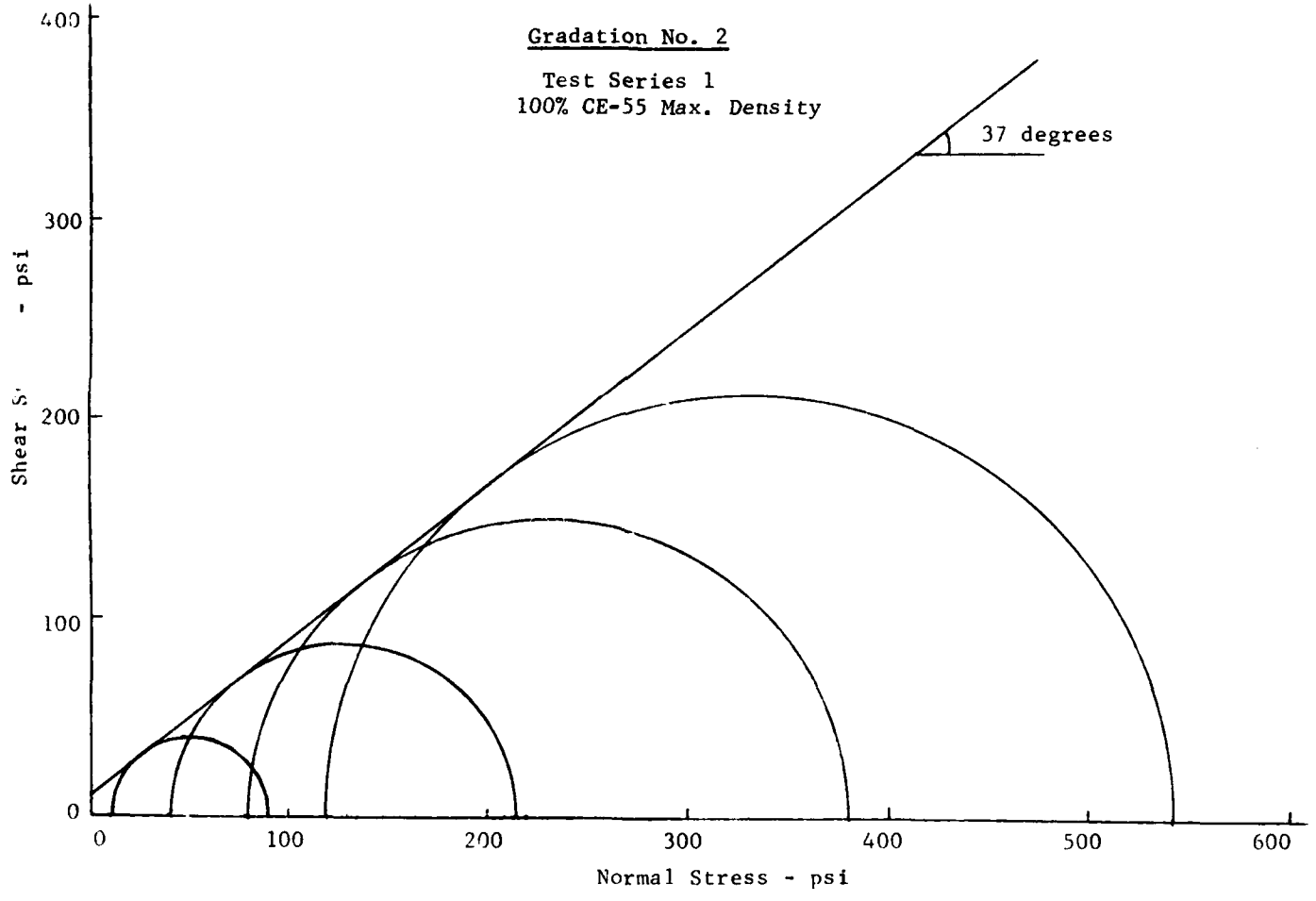

Fig. A-4 Mohr Failure Envelope for Gradation No. 2, 100% Max. Density.

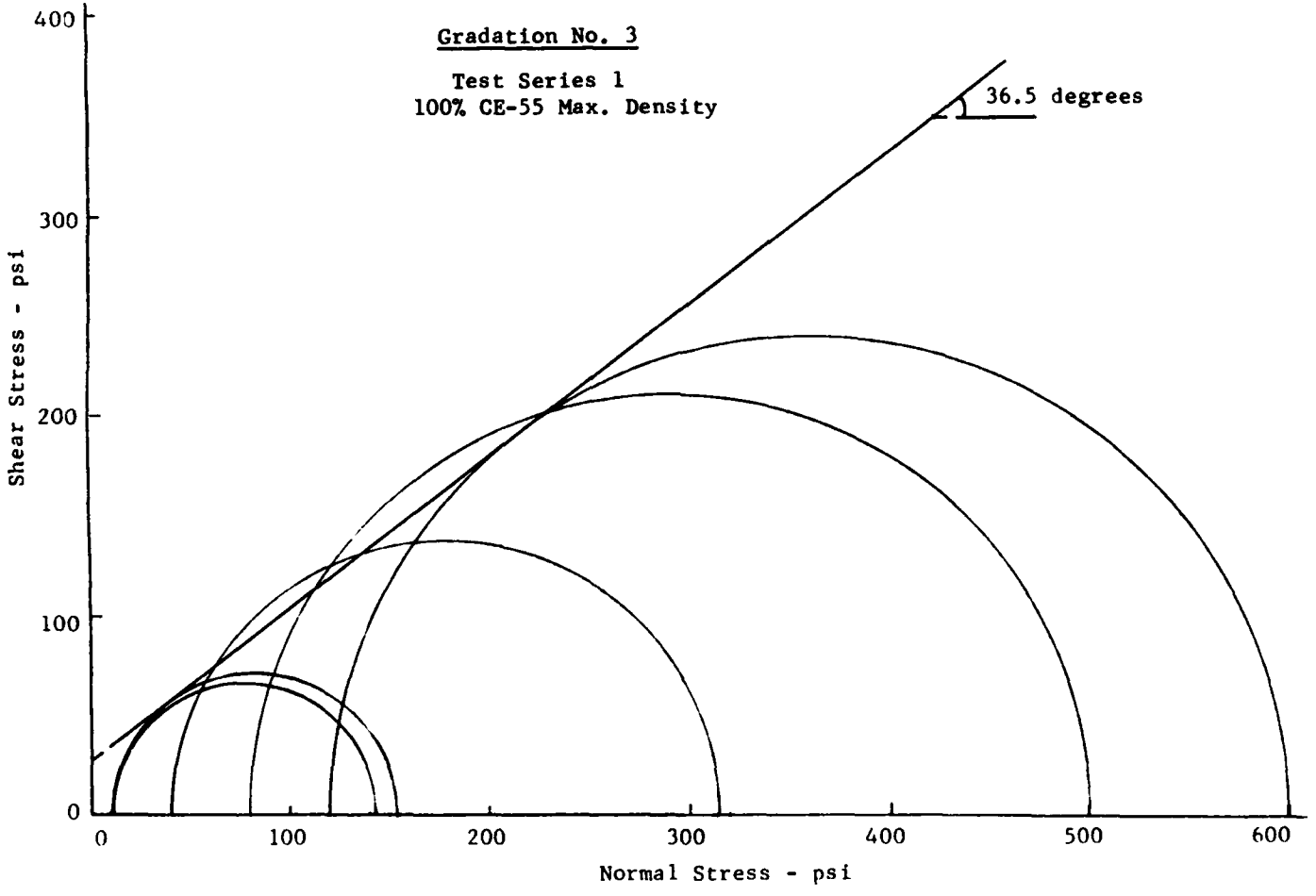

Fig. A-5 Mohr Failure Envelope For Gradation No. 3, 100% Max. Density.

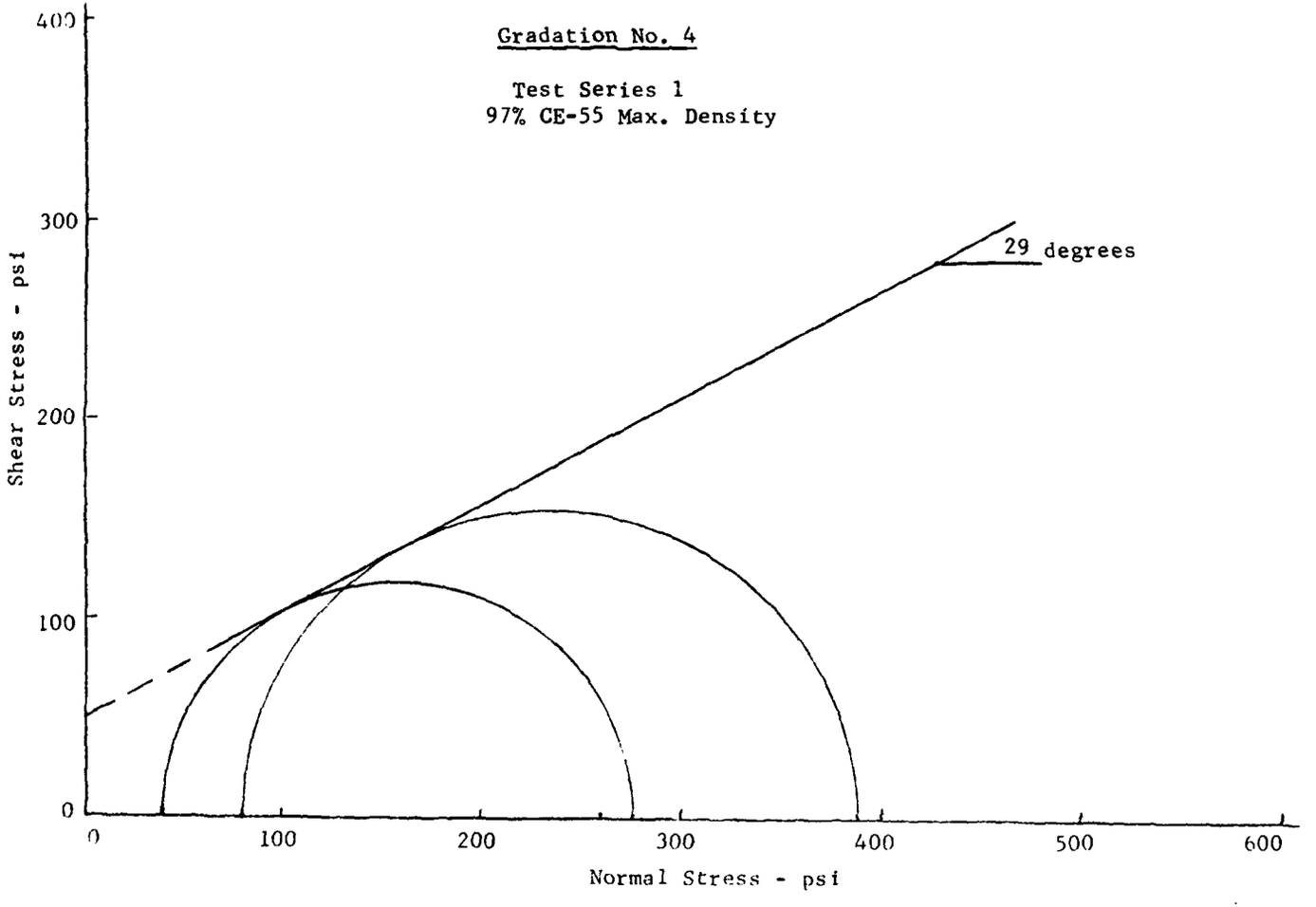

Fig. A-6 Mohr Failure Envelope for Gradation No. 4, 97% Max. Density.

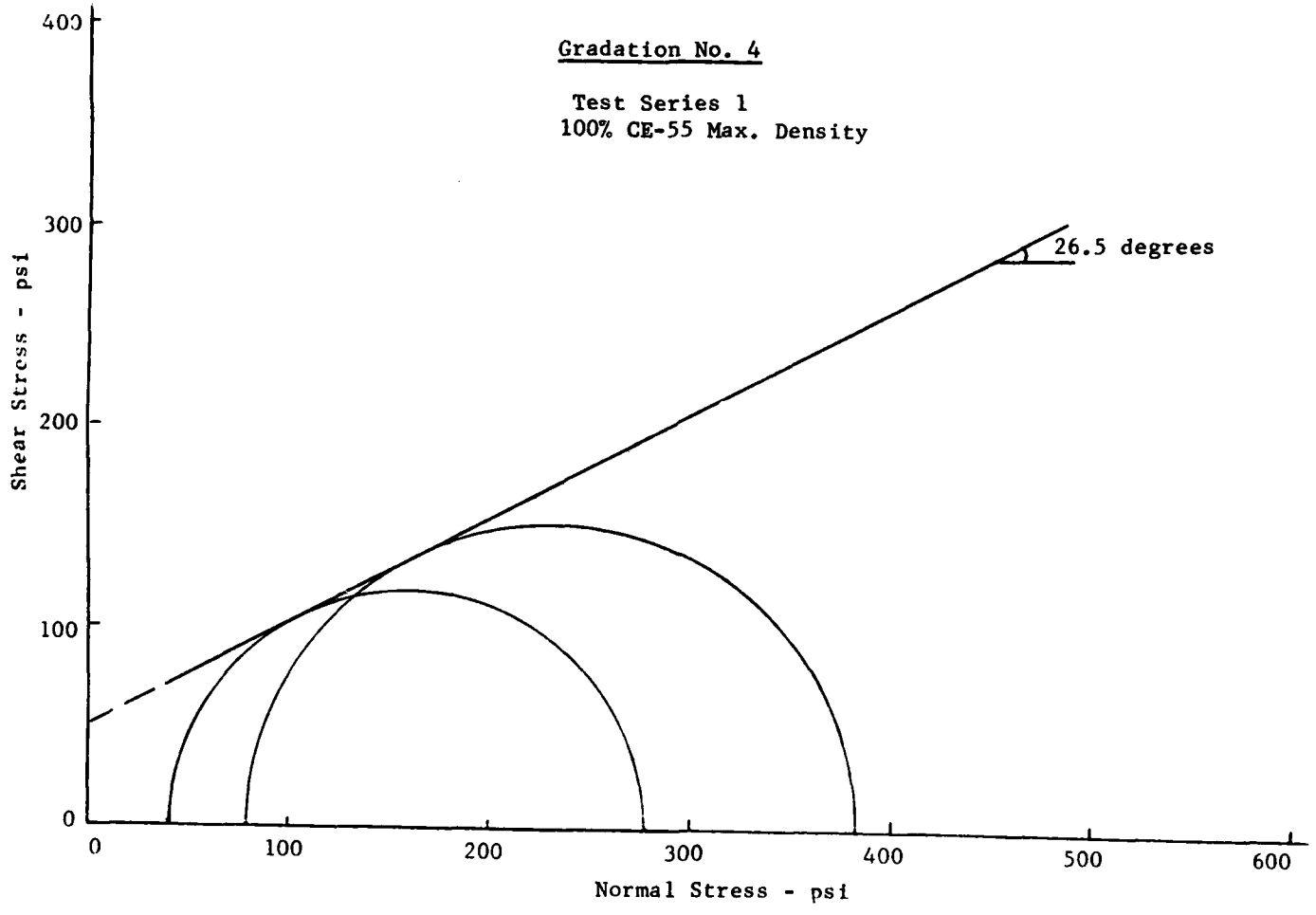

Fig. A-7 Mohr Failure Envelope for Gradation No. 4, 100% Max. Density.

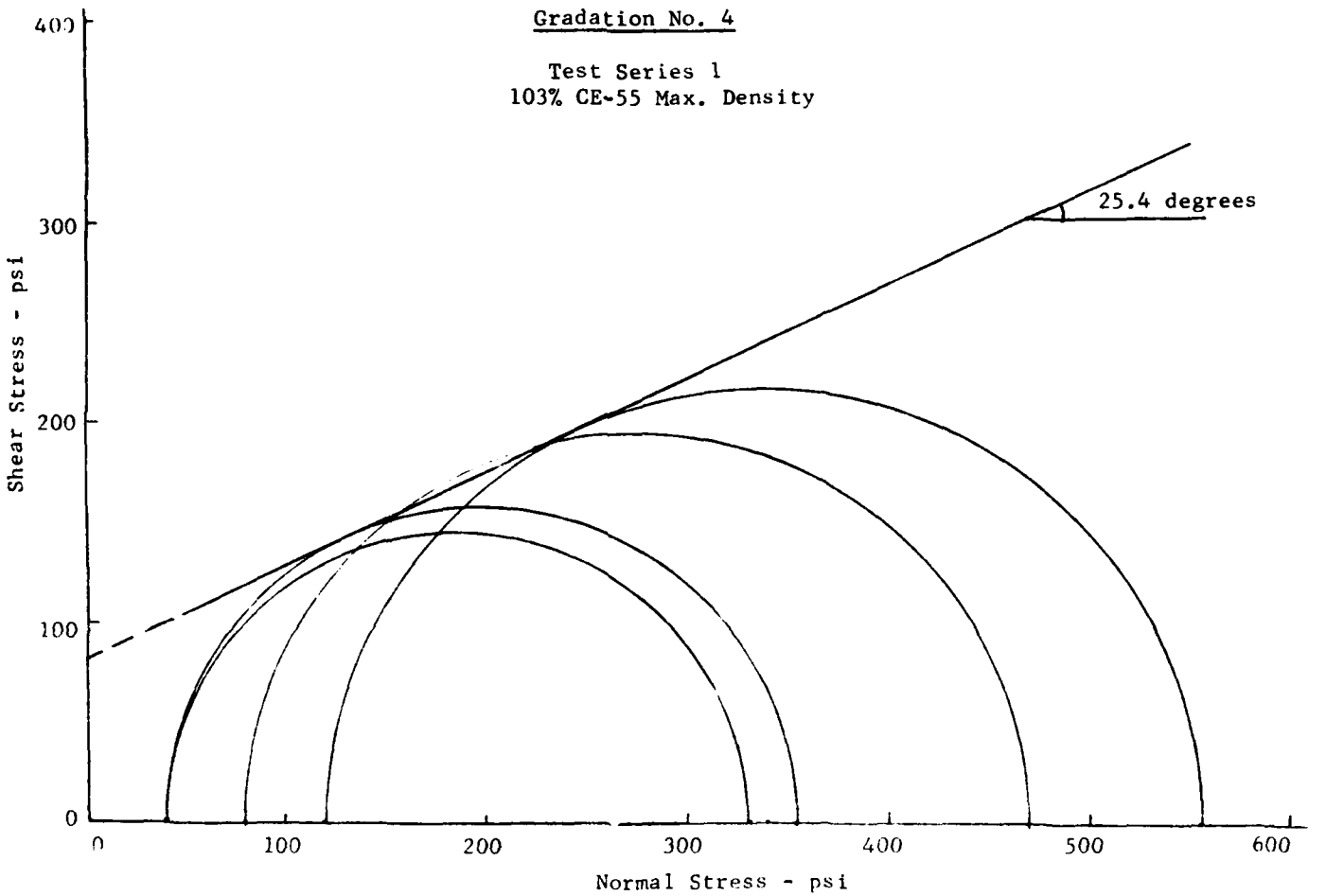

Fig. A-8 Mohr Failure Envelope For Gradation No. 4, 103% Max. Density.

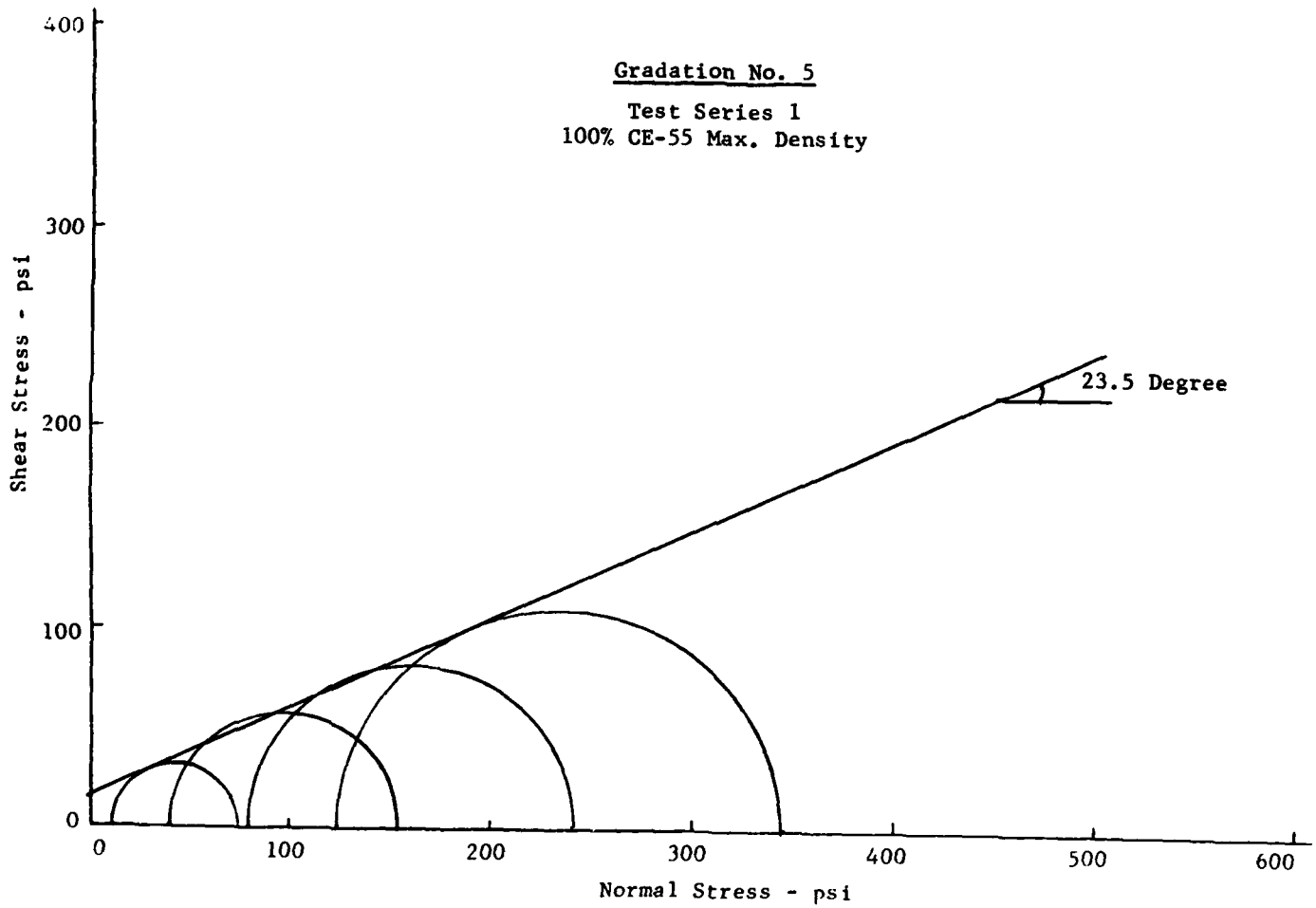

Fig. A-9 Mohr Failure Envelope for Gradation No. 5, 100% Max. Density.

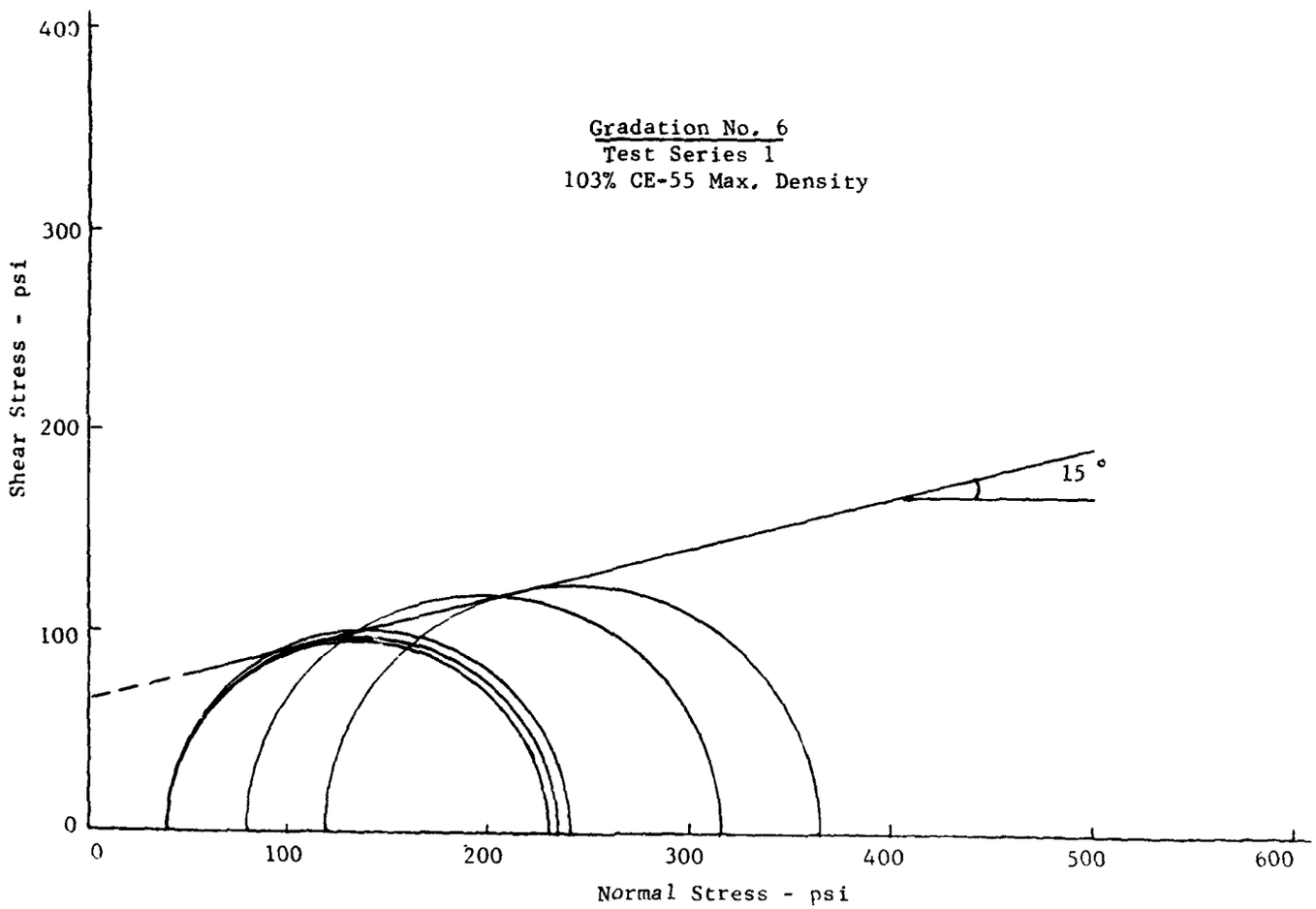

Fig. A-10 Mohr Failure Envelope for Gradation No. 6, 103% Max. Density.

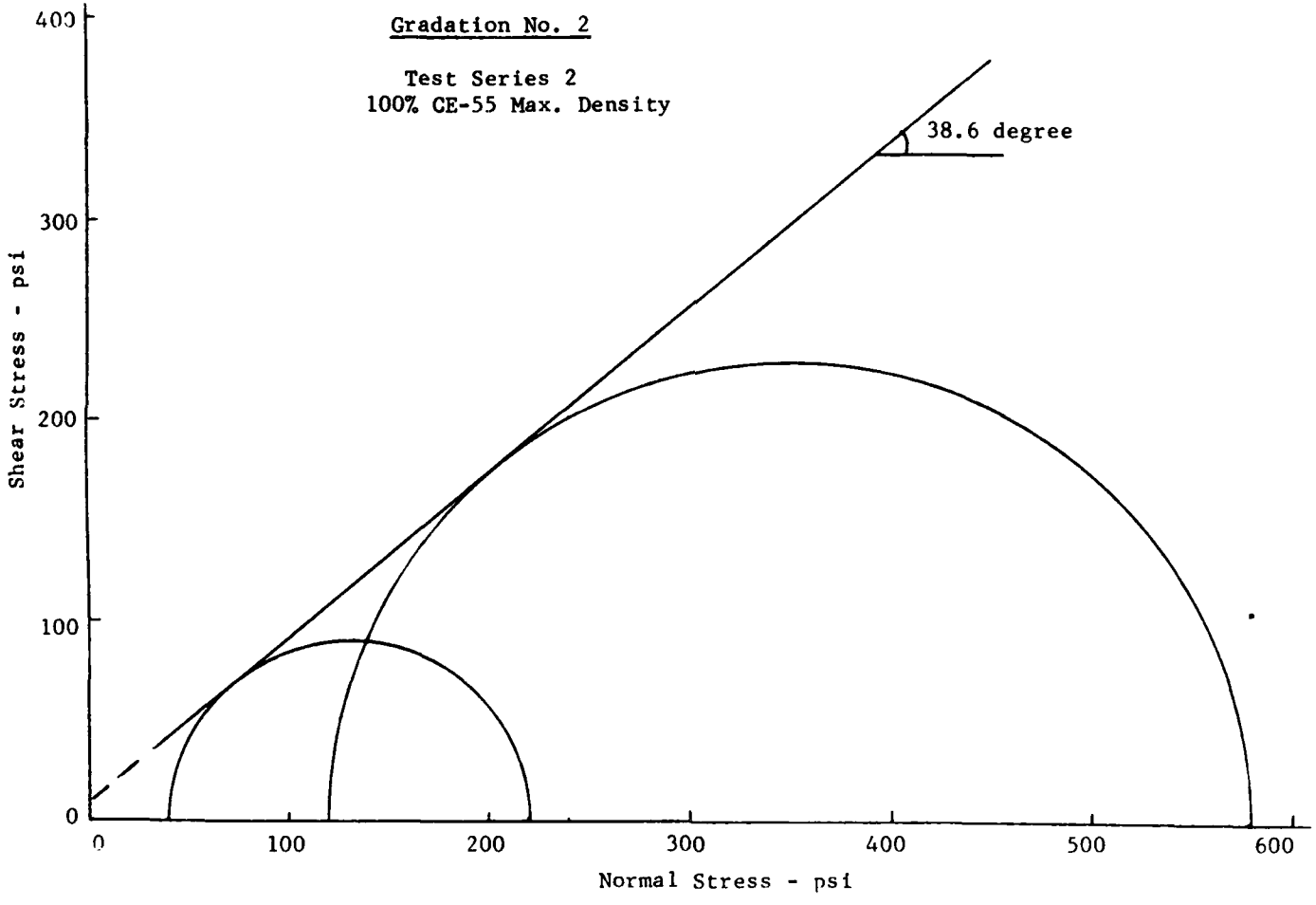

Fig. A-11 Mohr Failure Envelope for Gradation No. 2, 100% Max. Density.

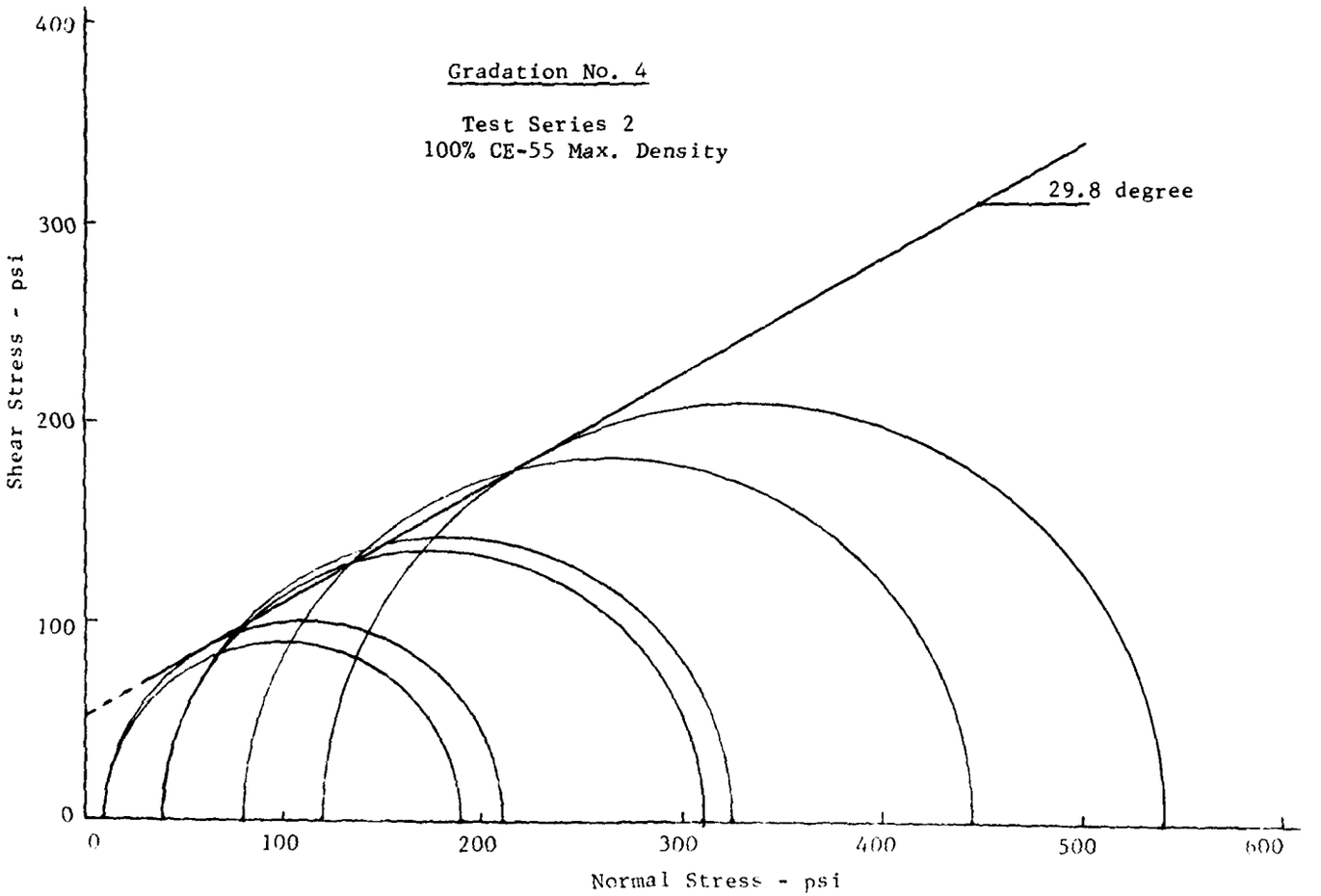

Fig. A-12 Mohr Failure Envelope for Gradation No. 4, 100% Max. Density.

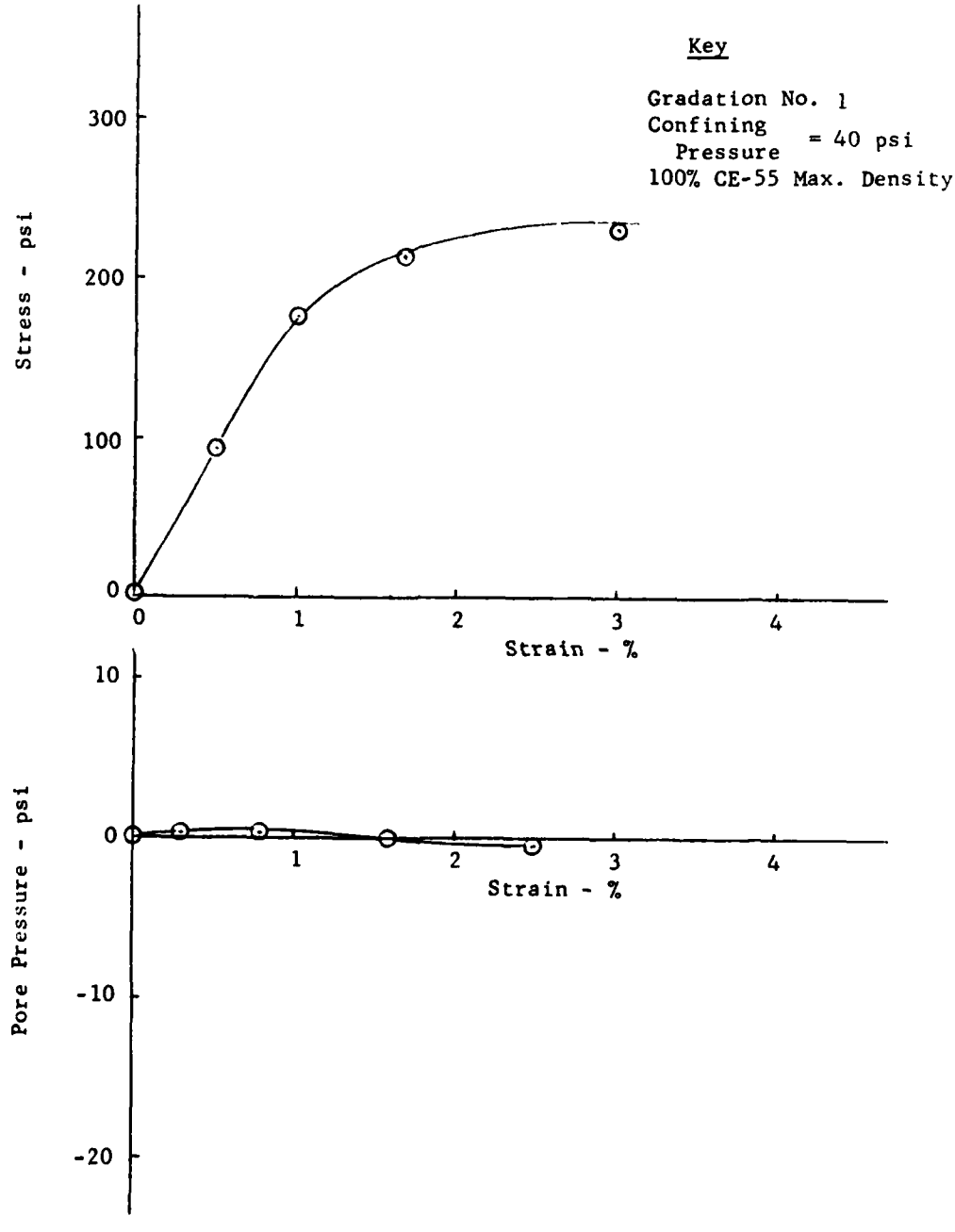

Fig. A-13 Typical Triaxial Test Data for Gradation No.1.

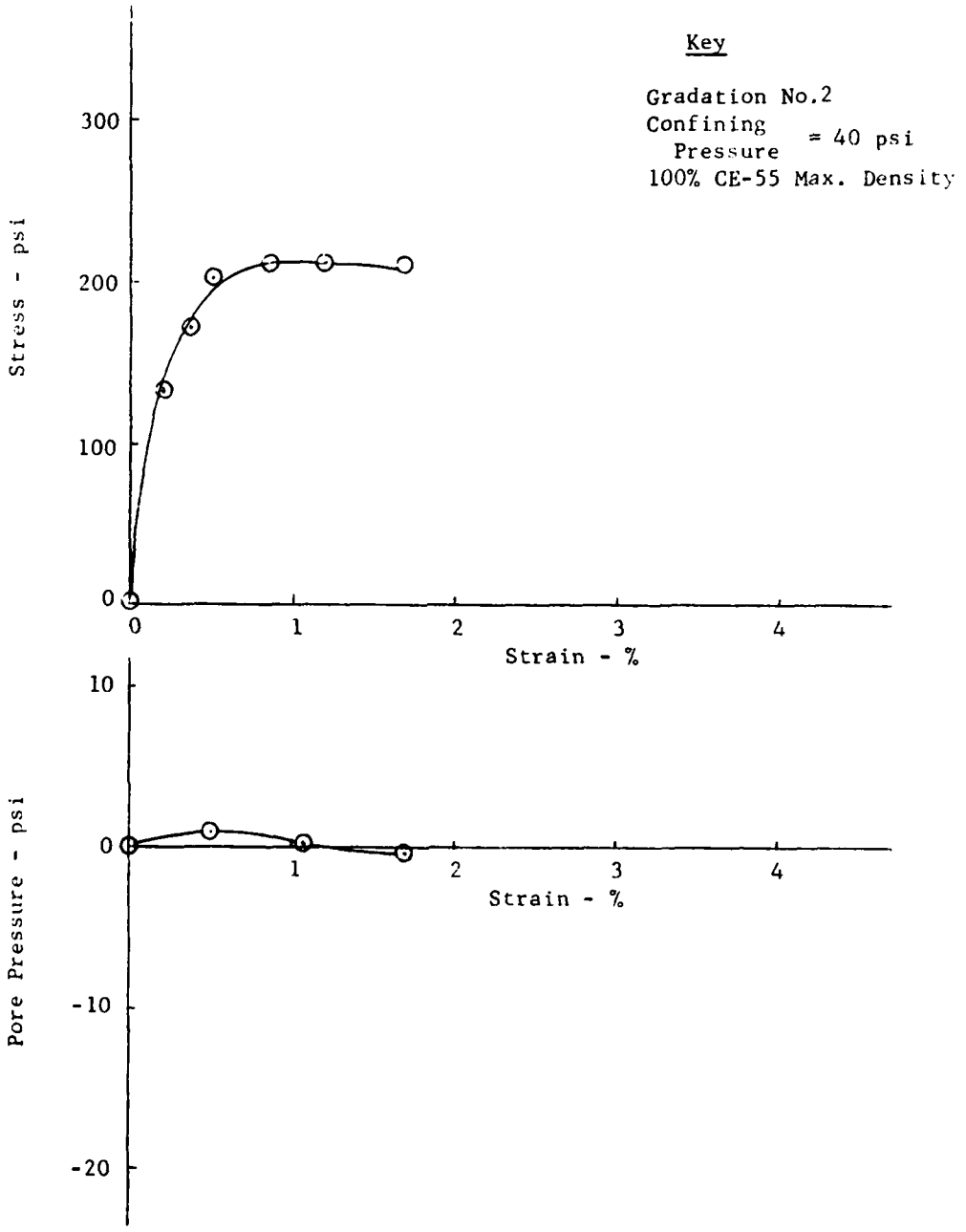

Fig. A-14 Typical Triaxial Test Data for Gradation No.2.

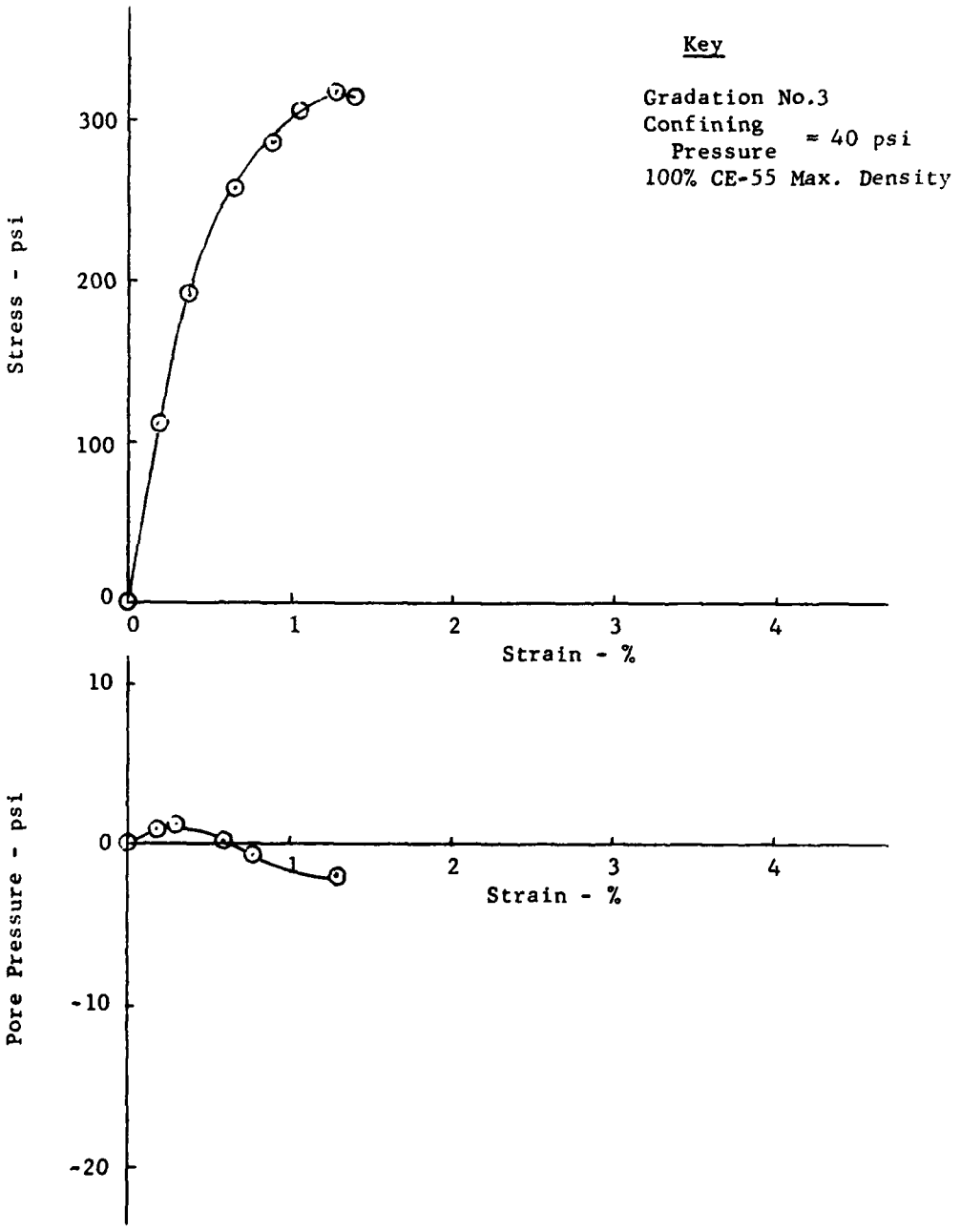

Fig. A-15 Typical Triaxial Test Data for Gradation No.3.

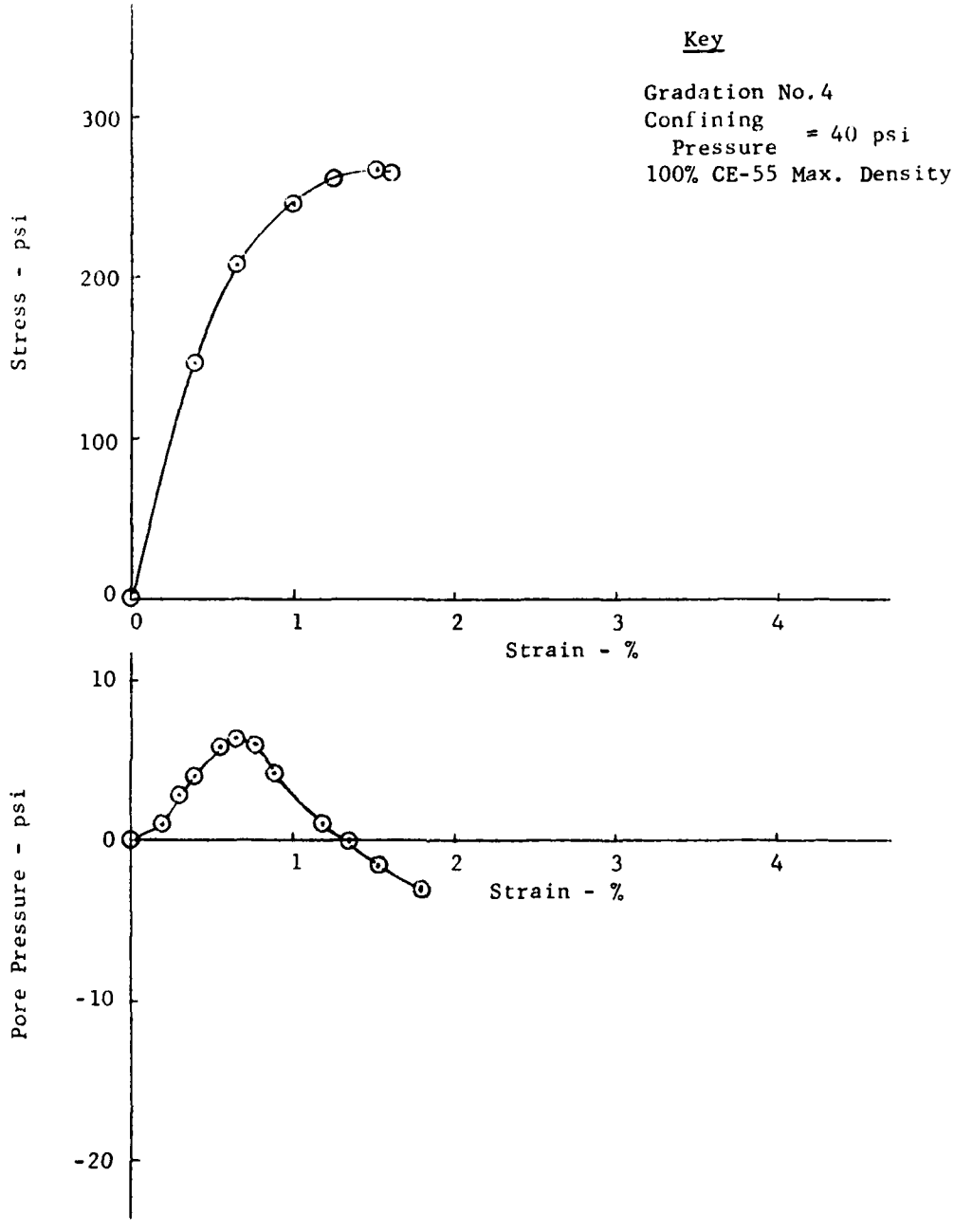

Fig. A-16 Typical Triaxial Test Data for Gradation No. 4.

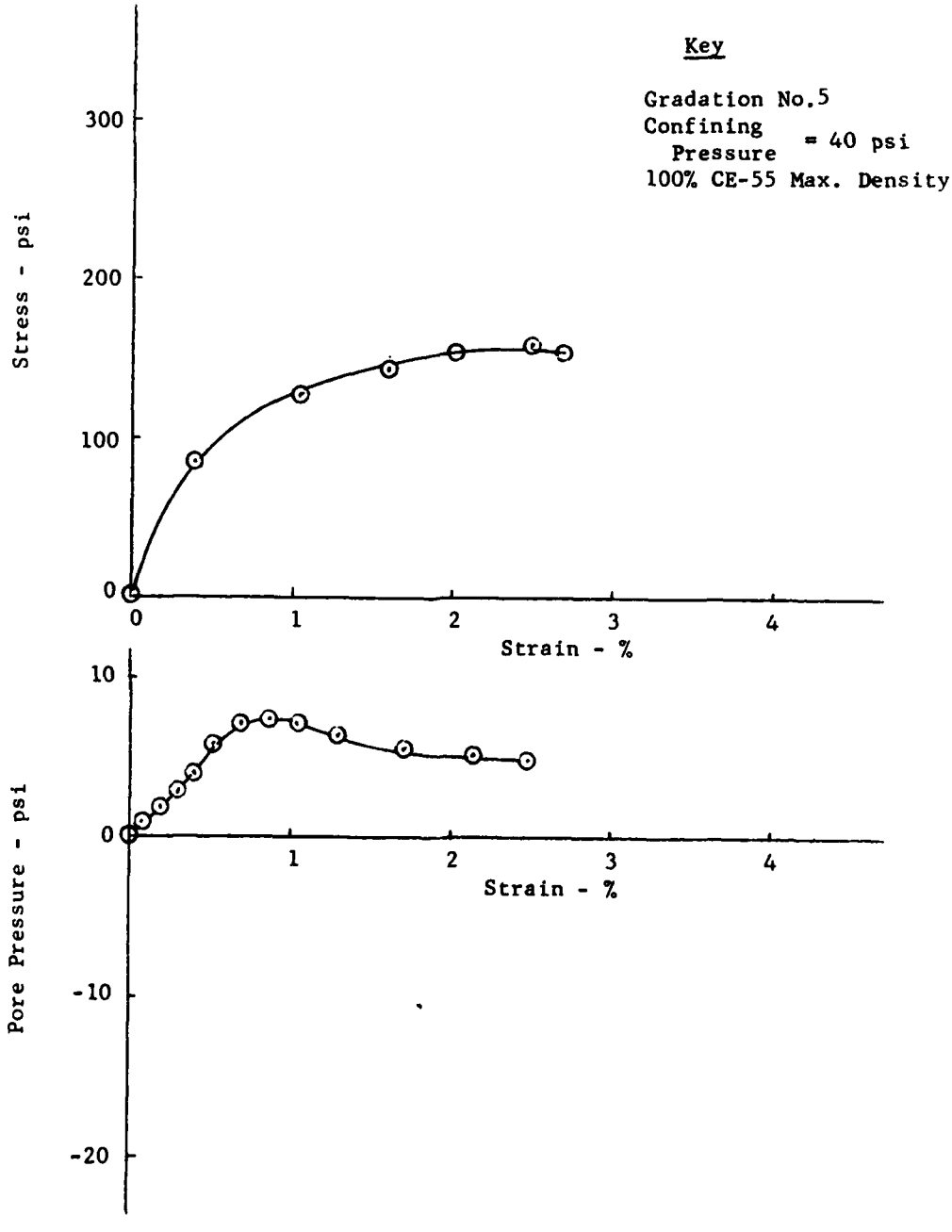

Fig. A-17 Typical Triaxial Test Data for Gradation No.5.

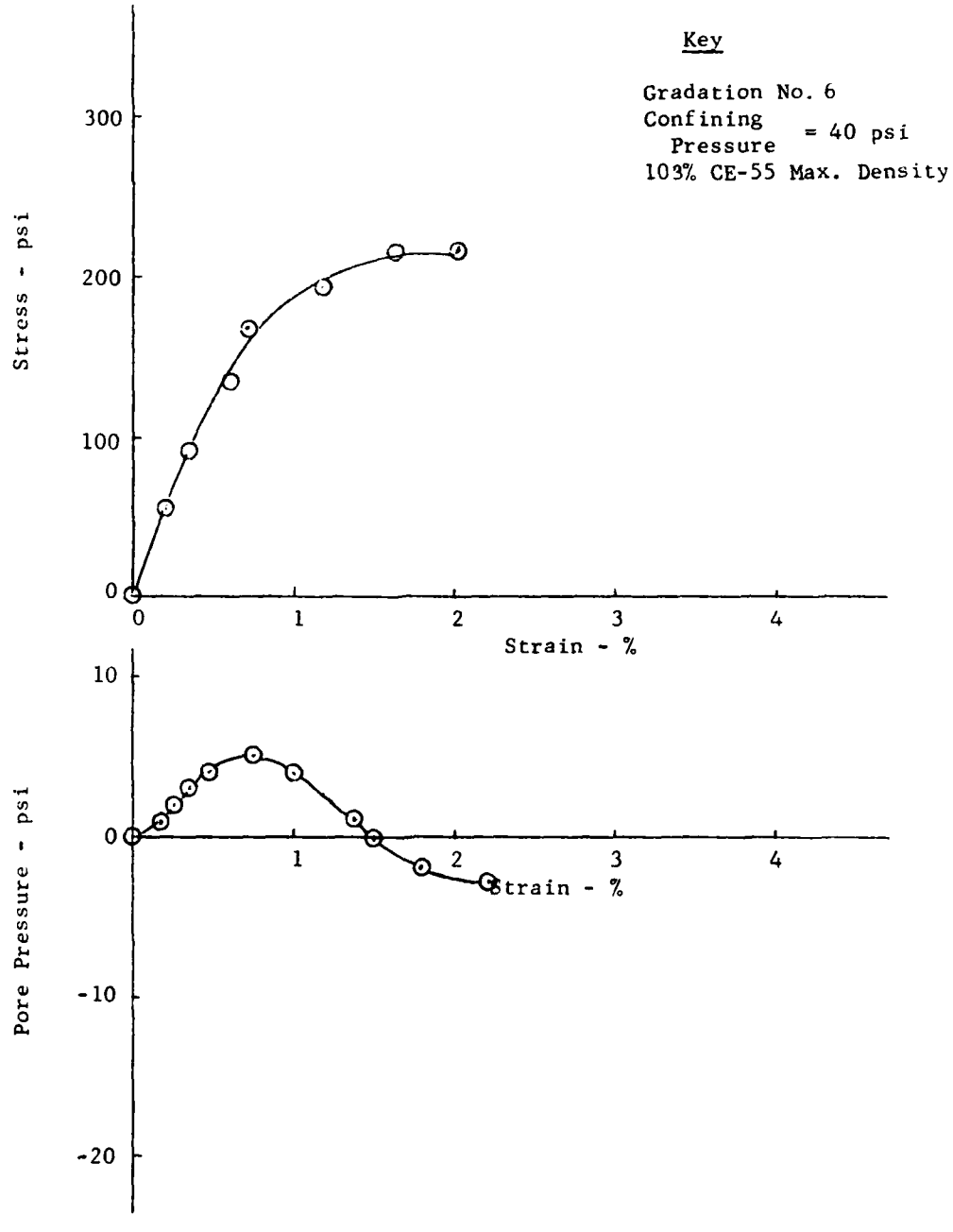

Fig. A- 18 Typical Triaxial Test Data for Gradation No.6.

LIST OF ACRONYMS

AFESC	Air Force Engineering and Services Center
ASTM	American Society for Testing Materials
BDR	Bomb Damage Repair
LVDT	Linear Voltage Displacement Transducer
NCEL	Naval Civil Engineering Laboratory
NCSA	National Crushed Stone Association
psi	pounds per square inch
WES	Waterways Experiment Station